Quark-Gluon-Plasma at Brookhaven and CERN

Thesis Submitted for the Degree of
Bachelor of Science
by

Fredrik Nordin

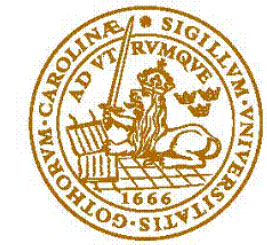

LUND
UNIVERSITY

DEPARTMENT OF PHYSICS

LUND, 2011

Abstract

For thousands of years we humans have asked ourselves the same question; what does our universe consist of and how does it work? One step in the direction to solve this mystery is to understand how the universe behaved just a few fractions of seconds after Big Bang. It is today believed that the matter present at this time consisted of a so called QGP. This is a kind of matter where the quarks and gluons are free from each other. If we can understand the QGP we might understand more about the laws of our universe.

This thesis is an easy-to-read introduction, appropriate for physicists not specialized in high energy physics, where I have gathered information to give a brief insight in subject QGP. The first few chapters contain general particle physics with a special weight towards the quarks, gluons and the strong interaction. Also proton-proton-collisions, nucleus-nucleus-collisions and their role in the hunt for QGP are discussed. In the latter chapters the discussion is directed towards the QGP. First we discuss what it is and how we can detect it. The two last chapters will briefly treat the experiments and the results. It should be mentioned that the experiments are being preformed as this thesis is written. At the moment, one of the more interesting things discovered is that the QGP behaves like a fluid, and not like a gas as predicted.

Contents

List of Figures

Acknowledgments

First of all I would like to thank my supervisor, Evert Stenlund, who made it possible for me to write this thesis. I appreciate all the encouragement and help I got from him. I am especially grateful for all the feedback I have gotten on my texts. Even though the texts not always were very good, Evert came with ideas and suggestions that made me satisfied and proud of them.

I also like to thank Anders Oskarsson for helping me with chapter 5, the chapter about accelerators and detectors.

Finally I would like to thank the Experimental High-Energy Physics division for letting me write my thesis there.

Chapter 1.
- The Standard Model

1.1 - Introduction

A dream many physicists have is a theory so fundamental that any other theory can be derived from it. No such theory has yet been developed, but in some aspects The Standard Model (SM) can be thought of as such a fundamental theory. This since it combines three of the four forces of nature, namely the electromagnetic, the weak and the strong force on a subatomic scale. To make the theory complete the gravitational force must be included as well, something that theorists currently are working on.
The development of The SM begun in the early 20th century, and was derived from quantum field theories. In these quantum field theories, like in almost all disciplines of physics, symmetries are very important. For example gauge symmetries and gauge transformation[1] is necessary to predict experimental results. To describe this mathematically one talks about *unitary groups* (U(n)) and *special unitary groups* (SU(n)). As a consequence of this, these groups are a very important part of the SM. But due to the abstract and complicated mathematics that is behind these issues, they will not be treated in this thesis. Instead some of the outcomes of the SM will be briefly discussed.

1.2 - Elementary Particles

According to the SM all particles are built up by a few fundamental *elementary particles*, i.e. particles without any substructure. There exist also a few particles that are responsible for the interaction between these particles. The first group is referred to as *fermions* while the second group is called *elementary bosons* (later referred to as bosons).

The fermions consist of 12 different particles (and their anti-particles). Half of the particles are called *leptons* and the remaining 6 *quarks*. A further partition of the fermions into groups is into generations. These generations can be seen in *Table 1-1* where the name and a few properties of the particles are indicated.

Fermions	1:st Generation	2:nd Generation	3:rd Generation	Charge (e)
Quarks	up quark (u) 2.34 ± 0.19 MeV/c^2	charm quark (c) ~ 1.3 GeV/c^2	top quark (t) ~ 170 GeV/c^2	+2/3
	down quark (d) 4.81 ± 0.14 MeV/c^2	strange quark (s) ~ 100 MeV/c^2	bottom quark (b) ~ 4 GeV/c^2	-1/3
Leptons	electron (e^-) 0.511 MeV/c^2	muon (μ^-) ~ 106 MeV/c^2	tau (τ^-) ~ 1.78 GeV/c^2	-1
	electron neutrino (ν_e) < 2 eV/c^2	muon neutrino (ν_μ) < 0.19 MeV/c^2	tau neutrino (ν_τ) < 18.2 MeV/c^2	0

Table 1-1: A table over the fermions. The lighter particles have been measured to a higher precision then the heavier, and so their mass is given more accurately [1].

Beside the information given in the table one should mention that all the elementary fermions have spin 1/2. From quantum mechanics this means that the fermions obey the Pauli Exclusion Principle. It says that no particles with spin 1/2 can occupy the same physical state

[1] An introduction to Gauge Theory will be presented in the chapter "The Strong Interaction", page 4.

within one system. This gives rise to e.g. shell structure in atoms, nuclei, quantum dots etc. The quarks do also have two other quantum numbers, namely baryon number and colour. All of the quarks have a baryon number of 1/3. Since the baryon number of a system must be an integer we have for example 1, 0 and -1 for a hadron, meson and an anti-hadron respectively. The total baryon number is conserved in all reactions. A consequence of this is e.g. that a proton can't decay into any other particle and should therefore be stable. This is in agreement whit experiments which have been preformed. In these a lower limit of the life time for a free proton is 10^{32} years. The other quantum number, colour charge, is the property that makes the quarks able to interact via the strong interaction (more on this topic later). It is this force that confines the quarks to baryons and makes it impossible to observe a free quark. All quarks have blue, green or red colour charge.

In the same way as the quarks have baryon numbers, the leptons have lepton numbers, L. Also this number is conserved in a reaction, but in this case also specific numbers for the different generations exists (leptonic family number, LF). Thus the electron and the electron neutrino have one LF called L_e, while the muon and the muon neutrino have another LF called L_μ. These LF are usually conserved and therefore the muon is most likely to decays into an electron, one anti-electron neutrino and one muon neutrino, see the reaction below.

	μ^-	$\rightarrow$	e^-	+	$\bar{\nu}_e$	+	ν_μ
L	1	=	1	-	1	+	1
L_e	0	=	1	-	1	+	0
L_μ	1	=	0	+	0	+	1

As we pointed out above the LF is conserved in reactions such as this. But a special case when this is not valid is for a free neutrino. This is due to the fact that the neutrinos can oscillate in so called neutrino oscillations. In a simplified model one can think of a neutrino as a combination of different kinds of neutrino states which changes in time. The time scale for this to happen is very long. This is shown in *figure 1.1*.

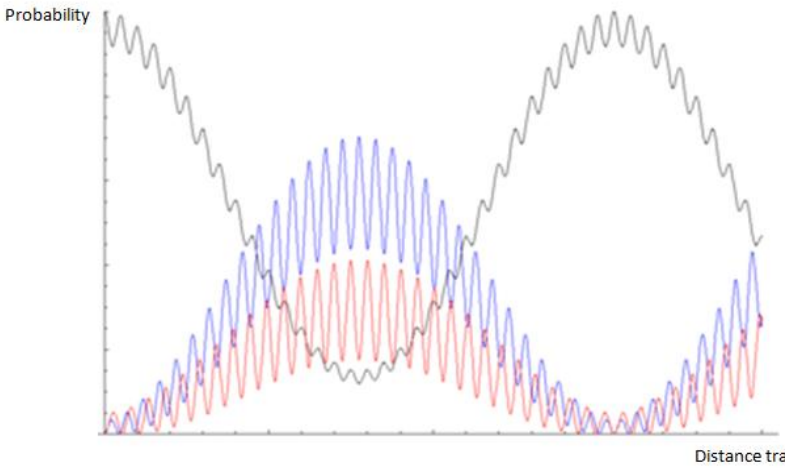

Figure 1.1: This graph shows the probability to find the neutrino in a state as a function of distance travelled. Here the initial state is an electron neutrino (black line). After some distance the probability to find the neutrino in a muon (blue) or tau (red) state is non-zero.

With this introduction to the fermions we can move on to the bosons. One fundamental difference between the fermions and the bosons is that bosons have integer spin (usually 1), so they do not obey the Pauli Exclusion Principle. A consequence of this is that all bosons in a

system can occupy the same state. In the SM there are currently several different kinds of bosons, the photons for the electromagnetic force, $W^{+/-}$ and Z for the weak interaction and gluons for the strong interaction. The theory also predicts the *Higgs boson* and the *Graviton* where the first one would give particles mass while the second would be the force carrier for the gravitation. These two particles have not yet been detected, and will not be discussed further. Since the strong force is such an important topic for this thesis it will be given an own section after the general introduction.

The range of the interactions is determined by the mass of the bosons. So the massless photons give an infinite range to the electromagnetic force, while the heavy $W^{+/-}$ and Z bosons give the weak interaction a short range. This relation is actually nothing else than Heisenberg's Uncertainty Relation;

$$\Delta t \Delta E \geq \frac{\hbar}{2}$$

A table containing the different bosons, their forces, range and charge is shown below.

Mediator	Force	Mass	Range	Charge
Photon (γ)	Electromagnetic	0	∞	0
$W^{+/-}$, Z^0	Weak	80,4; 91,2 (Gev/c^2)	~10^{-18}m	$\pm$1; 0 (e^-)
Gluon	Strong	0	∞	8 different colour charges[2]

Table 1-2: A table over the bosons.

When two or more particles interact they do so by emitting or absorbing elementary bosons. In fact also a free particle emits bosons all the time, but if no other particle is there to absorb them the particle have to absorb it itself. This means that particles are created and annihilated all the time. These particles are called virtual particles because they should not exist due to energy conservation. But as long as their lifetime (or rather lifetime with respect to mass) is short enough to obey the Heisenberg relation they are allowed to exist. The mass of the virtual particles is not necessary the same as for a normal particle. For example can a virtual photon have a non-zero mass. Sometimes the emitted boson creates two new particles. A photon could for instance create a pair of an electron and a positron. These two particles must however later annihilate to become a photon again, which the original electron could reabsorb. This is an example of a so called loop. So an electron for example, which can both interact both electromagnetic and weakly, is surrounded by a cloud of photons W^-- and Z-bosons (see *figure 1.2*).

[2] More about this in the next section.

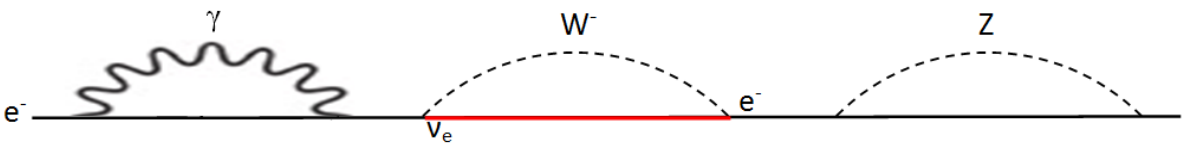

Figure 1.2: An electron emits and reabsorbs bosons. Note that the electron becomes an electron neutrino when a W^- is emitted. This is to conserve electric charge and LF. For the same reason the electron can't emit a W^+.

For simplicity the easiest forms of the emissions are shown there, but there could of course been lots of loops. In this figure we can also see that the weak interaction can change one particle into another. All these phenomena are called quantum fluctuations, and more information of that can be found in any introductory book on particle physics.

So if we now go back to the many particle interactions, we know that each of these particles is surrounded by a cloud of bosons. When e.g. two particles are close enough the particles doesn't have to reabsorb their own bosons. Instead they absorb each others, which mean that they interact.
Consider two electrons; in how many ways can they interact? First we have the emission of a photon from the first electron and absorption of the same photon from the second electron. This is the normal electron scattering. It could also occur via the exchange of a Z-boson. This exchange is however heavily suppressed by the electromagnetic interaction, not least because of the mass of the Z-boson (which makes the range short). The other two weak bosons on the other hand could not have been exchanged between two electrons. Again this is to conserve the electric charge and the LF. But if one of the electrons was another particle with the ability to interact weakly this could have been possible. A neutrino or a quark could e.g. been involved in such a reaction. A couple of the possible reactions that can occur can be seen in *figure 1.3*.

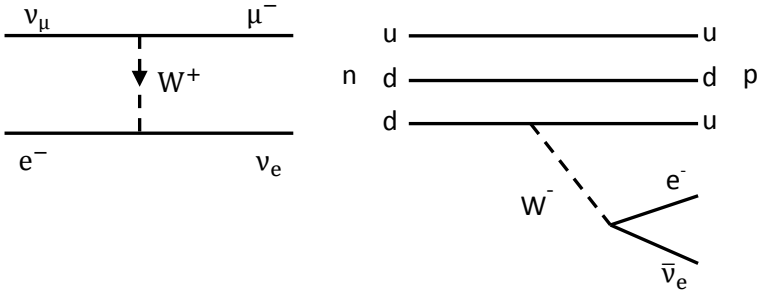

Figure 1.3: Two weak processes. The right one is known as beta-decay.

1.3 - The Strong Interaction

In the standard model the theory that describes and explains the strong interaction is called quantum chromodynamics (QCD). In some aspects this theory is similar to the QED, which describes the electromagnetic interaction. For example the strong force is mediated by a massless, electrical neutral spin-1 boson just like the electromagnetic force. In the case of the strong interaction the boson is called gluon, while called photon for the electromagnetic. One very important difference between the gluon and the photon is that the gluon both carries and can couple to colour charge. This is an important issue which give rise to phenomena such as jets, which will be treated in the next chapter. In the earlier parts of this thesis we gain some understanding for how particles interact, by emission and absorption of bosons. Before we

focus on the interactions from the view of the strong force, we need some more knowledge about the gluons.

The mathematics to derive the gluons is rather difficult, so here we just say a few words about how the problem is solved [2] and focus more on the actual results.
The field within this problem is solved is *Gauge Theory*. In this case Gauge Theory studies how the wave function of a physical object depends on the electromagnetic field acting on it. The point is that for any field with a special influence on the wave function there exist other fields with the same influences on the wave function. Let us for simplicity assume that we have a field described by **F**=(Φ,**A**) and the properties;

$$\boldsymbol{E} = -\boldsymbol{\nabla}\Phi - \frac{\partial \mathbf{A}}{\partial \mathrm{t}}$$

and

$$\boldsymbol{B} = \boldsymbol{\nabla} \times \boldsymbol{A}$$

Where E is the electric field and B is the magnetic field. Another field that would give the same electric and magnetic field as **F** is **F'**=(Φ',**A'**) where;

$$\boldsymbol{\Phi}' = \boldsymbol{\Phi} + \frac{\partial f}{\partial t}$$

and

$$\boldsymbol{A}' = \boldsymbol{A} - \boldsymbol{\nabla} f$$

In this case f is a scalar function. If we change **F** for **F'** it is called a *gauge transformation*. The two different potentials can now be put into the Schrödinger equation end set to be equal. After a bit of work one finds that the wave function actually gets a phase change under the transformation. But since the phase vanishes when probabilities is calculated the same physical state is described by the transformed and untransformed wave function. A wave function for which this is true is said to be *gauge invariant*.
In many applications it is appropriate to work the other way around. It is to demand that a state is gauge invariant and from that work backwards to find out how the potential and interactions look like. If this is done for the strong interaction one can show that the gluon comes in eight different colour states; these are shown below.

$r\bar{b}$ $\quad$ $b\bar{r}$

$r\bar{g}$ $\quad$ $g\bar{r}$

$b\bar{g}$ $\quad$ $g\bar{b}$

$$\frac{1}{\sqrt{2}}(r\bar{r} - b\bar{b}) \qquad \frac{1}{\sqrt{6}}(r\bar{r} + b\bar{b} - 2g\bar{g})$$

As we can see here the gluon always carries one colour and one anti-colour. So when a quark emits a gluon, the quarks changes it owns colour. For example could a blue quark emit a blue and anti-green gluon and become green. Furthermore, a red quark could absorb an anti-red and green gluon and become green. The two processes are shown in *figure 1.4*.

Figure 1.4: Two interactions in which the quarks change their colour.

Another consequence of the fact that the gluons carry colour charge is that they can interact with each other, in so called gluon self-coupling. This gives rise to two of the quarks' characteristic behaviour, *asymptotic freedom* and *confinement*. Thus the quarks in a hadron are basically free as long as the distance between them is short enough (the radii of the particle). But when the distance gets large the quarks seems to be bound to each other (or confined to the particle).
The last thing we will cover here is *sea quarks*. These are quarks that can be created from a gluon, within the time-energy relation given by Heisenberg's Uncertainty Relation. Due to conservation laws it is always a quark and its anti-quark that is produced. I most case it's the lightest up or down quark-pair that is produced. With this in mind we cannot always think of baryons as a particle consisting of 3 quarks. Instead we must see the baryon as a superposition of 3 *valence quarks* (the normal quarks), gluons and quark anti-quark pairs. In the chapter about proton-proton collisions we will see what consequences this will have.

1.4 - Jets

Before we discuss the important subject concerning jets it is good to explain the process called fragmentation, also called hadronization. One model that describes the hadronization process is the string model. To briefly explain this model we can first think of two charged particles and their properties, and later do the same for two colour charged particles. So if we have one electron and one positron a distance apart there will be an electric field between them. The strength of the field is proportional to the density of field lines. When the particles are separated the field lines spreads out in space and the field gets weaker, see *figure 1.5*.

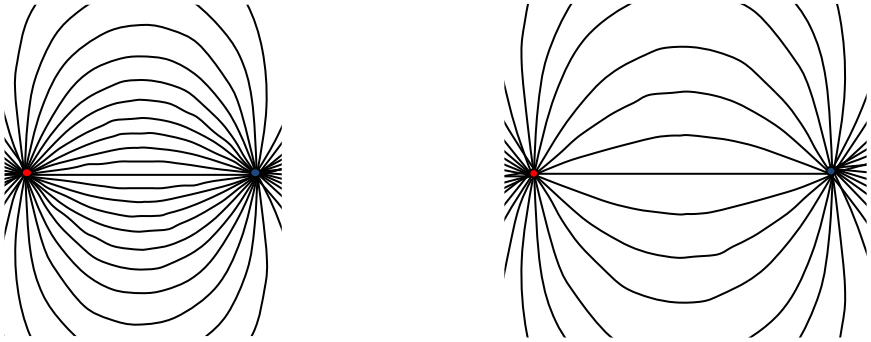

Figure 1.5: Here is the field between two particles with opposite charges. As the particles are separated the field gets weaker.

The idea of a field between electrically charged particles can be directly translated to colour charged particles, in other words there will be a colour field made up by gluons between the quarks in a hadron. To make it easy one can think of a meson which consist of a quark and an anti-quark. Also here the strength of the field is proportional to the field line density, but there is one fundamental difference. When the quarks are moved apart we don't expect the field to become weaker since the quarks are confined to the hadrons. The string model's explanation to this that the gluons can couple to each other (this is not possible for the electric field which is made up by photons). So when the quarks are separated the field line density is unchanged since the interaction between the field lines via gluons holds them together. The more the quarks are forced apart the more gluons are exchanged between the field lines and the do for that reason not spread out in space, see *figure 1.6*. To treat this phenomena mathematically one usually approximate the colour field by a mass less relativistic string in one dimension. Sometimes this string breaks up in two. For example can this happen if a pair of quarks (quark and anti-quark) is created by quantum fluctuations. This pair will then be affected by the colour field made up by the "old" quarks and pulled apart until two new quark pairs are created. These two new pair consists both of one "old" and one" new" quark. If the energy in the string between the originally quarks was very high, the two new pair will be pulled apart as well. This means that the same process might happen again, so that even more new pair can be created. This can go on as long as the energies in the strings are sufficient to create new quark pairs. It is this particle producing phenomena that is called hadronization.
In the example explained above only mesons are produced, but experiments have shown that also baryons can be created. This can happen if both a di-quark and an anti-di-quark are created by fluctuations at the moment when the string breaks. In this process both a baryon and an anti-baryon are created, which means that the baryon number is conserved.

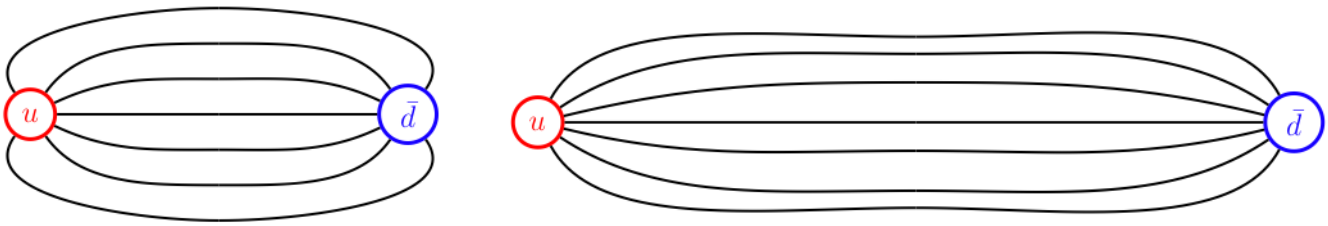

Figure 1.6: Here we can see that the gluons hold the field lines together as the quarks are separated.

To approach the theory of jets one can first think of an experiment where an electron and a positron collide. Since the two particles are each other's antiparticles they will annihilate and become energy. If the energy in this annihilation is greater than the rest mass of two quarks, there is a possibility that a quark-anti-quark pair is produced. If this happens at even higher energies the two produced quarks are ejected out of the creation point. Since the momentum must be conserved in this process the two quarks must have transverse momentum of the same magnitude, but in opposite directions. Because of this the quark pair split up. This separation of quarks is basically the same process as explained from the view of string model above. So what will happen is that when the created quarks in the pair are separated they will fragment. In a detector this will look like two showers of hadrons with origin in the collision point of the electron and positron. A picture of this can be seen in *figure 1.7*. Each of these two hadronic showers is called jets and this phenomenon is called a two jet event. As a matter of fact there is a possibility that a three jet event can occur. For this to happen, one of the fragmenting quarks must emit a high energy gluon before it fragments. Since also the gluon will fragment three jets will be detected. In the detector this will be detected as one stronger signal and two weaker. The strong signal corresponds to the quark that did not emit the gluon, while the two weaker are the other quark and the gluon. Due to conservation of momentum the quark recoils when the gluon is emitted. So the spatial appearance in the centre-of-mass frame will be one jet in one direction, and the sum of the other jets in the opposite direction, *figure 1.8*. Events with more than three jets can also occur, but with decreasing probabilities as the number of jets increases. [3]

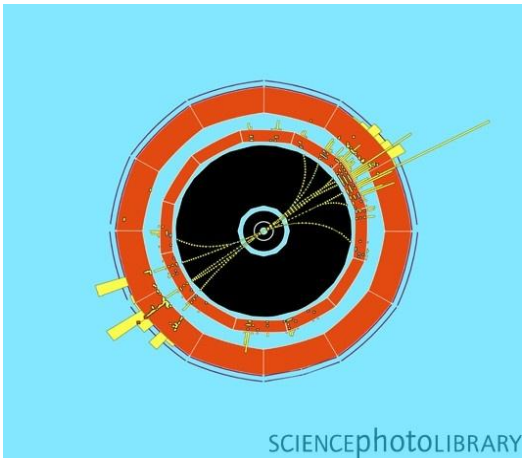

Figure 1.7: A two jet event detected after the collision between a positron and electron at CERN. The intermediate particle in this case was a neutral Z-boson, which later decayed into a quark-anti-quark pair.

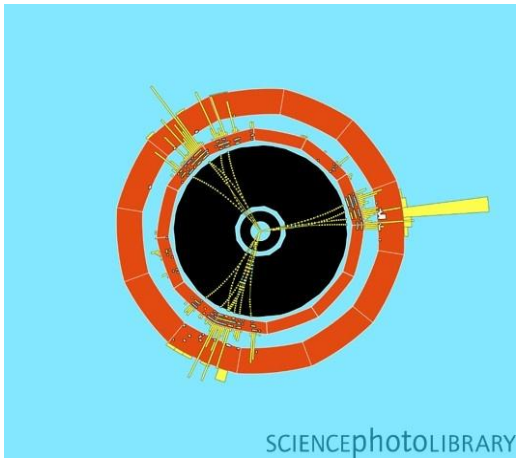

Figure 1.8: A three jet event, also detected at CERN after a collision between a positron and an electron. In this case one of the quarks emits a gluon before it fragments which results in an additional jet.

Chapter 2.
- Proton-Proton Collisions

2.1 - Introduction

In many aspects the collision between two protons is more complicated than between an electron and a positron. To think of the electron and positron as point particles without any internal structure is for example possible (and by today's knowledge correct), but this is not true for the protons. For the protons it is necessary to incorporate the quarks and gluons in the theory that describes the collisions. So instead of a two particle problem we now have a problem with two systems, each system with three valence quarks, sea quarks and gluons that interact in a complicated way. So before we try to understand the proton-proton collision we will try to understand how we can look into one single proton.

2.2 - Scattering of Hadrons

To investigate how the internal structure of a very small object looks like, we can send particles against it and see how the particles scatter. This is the same idea that Rutherford had in 1911 when he in an experiment accelerated alfa-particles against a gold foil. Since the alfa-particles scattered in a random angle (but mainly 0° from the beam direction) he could conclude that the atom is mostly empty space, but that there also should be a heavy nucleus surrounded by electrons. If we like to do the same experiment for a proton we have to increase the beam energy. This is because the resolution λ is given by the relation

$$\lambda = h/p$$

where p is the momentum. In experiments like this the most common particles to produce beams of is some kind of leptons. This is because they are most likely to interact electromagnetically with the proton and because they are point-like. Both of these properties make the calculations easier. There are two types of scattering processes; the elastic and the inelastic scattering. The elastic scattering was e.g. used to measure the mean radius of a proton. In this case the experiment is very similar to the Rutherford experiment and the leptons bends in different angles due to the protons charge distribution. But if we want to investigate the inner structure of the proton, then inelastic scattering is the method to use [2].

As said before the scattered particle is usually a lepton, so let us here assume that we are dealing with an electron. In the initial state the electron have energy E and momentum **p** while the hadron it is scattered against (let us say a proton) have energy E_p and momentum $\mathbf{p}_p$. If the electron is accelerated against the proton it will at some point interact with it. Almost all of the interactions will be electromagnetic and mediated by a photon with momentum **q**. In order to resolve the quark structure inside the proton **q** must be large. Thus in the final state, the electron will have a lower energy E' and a lower momentum **p**'. In almost all of the processes the photon is absorbed by a quark that gains high enough energy to escape from the proton. Hence both the escaped quark and the 2 remaining quarks fragment in a way that was described in *section 1.4*. A picture of this process can be seen in *figure 2.1*.

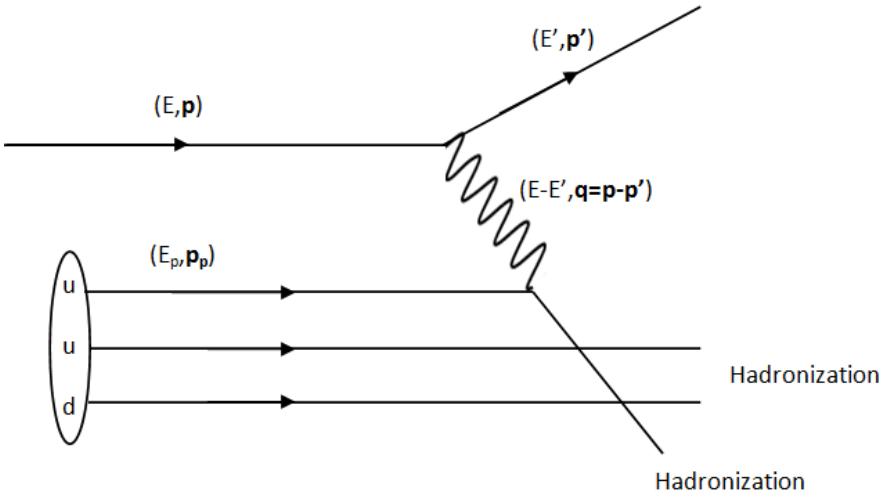

Figure 2.1: Here an electron scatters against a proton.

To simplify the calculations of this reaction it is convenient to define x by

$$x = \frac{Q^2}{2M\nu}.$$

Here M is the mass of the proton, ν the energy difference between the electrons initial and final state and Q, the Lorentz invariant momentum transfer, is defined by

$$Q^2 = (\boldsymbol{p} - \boldsymbol{p}')^2 - (E - E')^2.$$

The variable x is called the *Bjorken parameter* or *scaling parameter*. The values of x lies between 0 and 1 and is often thought of as the part of the protons total momentum carried by one single parton[3].

To estimate the cross-section between two particles (where at least one is a hadron) the variable x can be used to form the *structure function*. It is usually denoted F(x) and is in some aspects like a probability distribution over how probable it is to find a parton carrying a specific momentum, x·**P**, of the hadrons total momentum. Since the hadrons not only consist of the valence quarks, but also gluons and sea-quarks, the peak of the distribution is concentrated to lower values of x instead of **P**/3 which it would if there only existed 3 valence quarks. This is because the sea-quarks and the gluons also carry a part of the hadrons momentum. When x reaches 1 the structure function more or less vanishes, see *figure 2.2*.

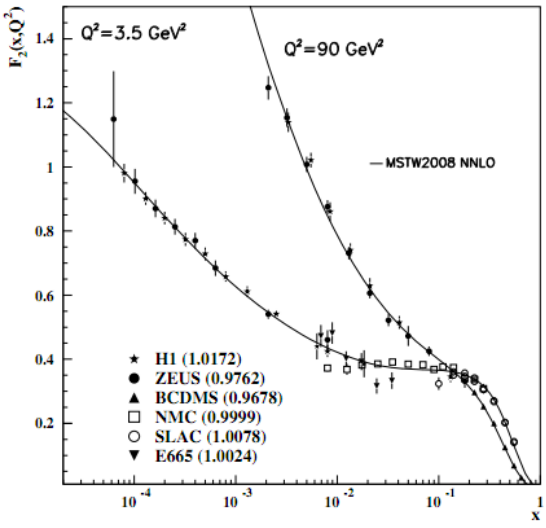

Figure 2.2: The structure function for a proton.

[3] Partons are the constituents of the baryons, either a quark or a gluon.

In *figure 2.2* it is also obvious that the structure function depends on Q^2. This is because Q^2 is the parameter we change to look deeper inside the hadrons internal structure. At lower values of Q^2 the emitted photon will most likely scatter against one of the valence quarks, but as Q^2 grows the probability to interact with a sea quark becomes larger.

Even though the structure functions won't be used in any larger extent in the following parts of this thesis they are of great importance when cross sections are calculated. However, this is one of the major steps when going from collisions between leptons to hadrons.

2.3 - Proton-proton Collisions

2.3.1 – Variables in Collisions

In the collisions we will discuss here, between two protons and later two nuclei, the velocities of the beams are very close to the velocity of light. They are therefore highly relativistic and the calculations of properties such as velocity, momentum and kinetic energy become more complicated than for particles at lower velocities. One problem is e.g. that the velocities are no longer additive. To go around this problem a new property called *rapidity*, y, has been defined [4] according to

$$y = \frac{1}{2}\ln\left(\frac{E + p_z}{E - p_z}\right) = arctanh(\beta).$$

Here E is the energy and p_z the momentum in the beam direction, along the z-axis. An important feature of the rapidity is that it is additive, even at relativistic velocities. And when the particles speed decreases to none-relativistic velocity, it smoothly approaches the velocity in units of the velocity of light. From the definition above it is simple to find

$$E = m_t \cosh(y)$$

and

$$p_z = m_t \sinh(y).$$

These two equations are useful when changing between the rapidity and the energy and the momentum. In the equations a new form of mass appears, the *transverse mass* given by

$$m_t^2 = m^2 + p_t^2.$$

Even though the rapidity seems to be easy to calculate, it may sometimes be hard to measure both the energy and the momentum (needed to express the rapidity). Therefore another, easier measured, quantity has been derived as well, namely the *pseudorapidity*. The formula for the pseudorapidity can be derived from the rapidity formula under the assumption that the momentum is large compared to the mass. The notation of it is η and it is given by

$$\eta = -\ln\left(\tan\left(\frac{\theta}{2}\right)\right)$$

or

$$\eta = \frac{1}{2}\ln\left(\frac{|\boldsymbol{p}| + p_z}{|\boldsymbol{p}| - p_z}\right).$$

In these equations it is enough to measure either the angle, θ, between the beam axis or the absolute value of the momentum and its z-component. If one wishes, it is possible to go from pseudorapidity to rapidity via the formula

$$y = \frac{1}{2}\ln\left(\frac{\sqrt{p_t^2\cosh^2(\eta) + m^2} + p_t\sinh(\eta)}{\sqrt{p_t^2\cosh^2(\eta) + m^2} - p_t\sinh(\eta)}\right).$$

2.3.2 – The Collisions

Now when the variables are defined, we can discuss how the collisions work. We will begin in a classic manner with the *Lund String Model*. This is the same model that we used to explain jets in section 1.4. Now, however, we have to extend the theory from lepton collisions to hadron and even nuclei collision.

The first step is to think about a hadron (now a baryon rather than meson) as a system of three valence quarks coupled by strings [5], as in *figure 2.3*. When two such hadrons collide, their colour fields over-lap and might couple to each other, resulting in an elongated (sometimes called excited) hadron more looking like a quark and a di-quark connected by a *colour string*, see *figure 2.4*. In this example the quark has lost much of its momentum, while the di-quark basically has the same momentum as before the collision. The single quark is therefore called wounded.

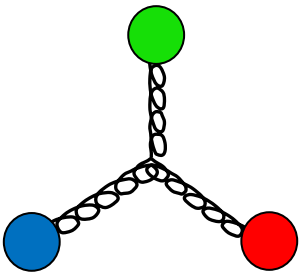

Figure 2.3: An arbitrary baryon in the string model

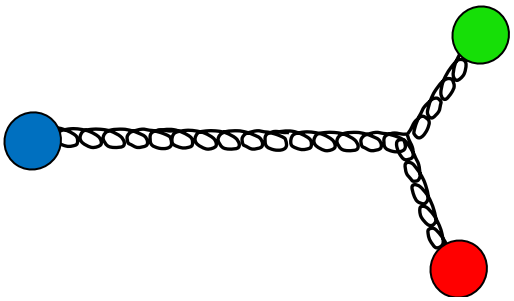

Figure 2.4: A baryon that been elongated after a collision with another baryon.

From the conclusions in section 1.4. we know that the quark di-quark is not a stable object, since it can be seen as two colour charged particles (which are not allowed to exist). And in accordance with that it fragments into hadrons which later can be detected. In a more advanced description of the above described process, phenomena like colour ropes can be observed. That is when two colour strings fuses together into one string. But the simplified model is enough to proceed in this thesis.

The center-of-mass energy in pp-collisions ranges from a few GeV up to several TeV. The inelastic cross section for the higher energies is around 30mb. There is also a cross section for an elastic collision to occur, but in these collisions no interesting (for our purpose) physics

occur. This is due to the fact that the energy realised in the collisions is the energy that produces the new particles that we are interested in. The total number of all produced particles is called *multiplicity*. This quantity counts both charged and uncharged particles. This is in reality hard to measure, since the uncharged particles are tricky to measure. So instead it is common to talk about the *charged multiplicity*, which then is just the total of all the charged particles produced. If the charged multiplicity is plotted versus the rapidity (or more often pseudorapidity) at low $\sqrt{s}$ one finds that the curve will get a bell-like shape, *see figure 2.5*.

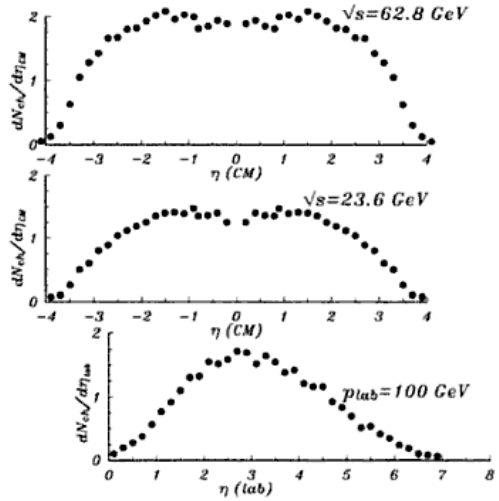

Figure 2.5: The multiplicity as a function of the pseudorapidity. The lower plot is from a collision where $\sqrt{s}$ =13.8 GeV. In this plot the pseudorapidity is measured in the reference frame of the lab, whiles the two other, at higher energies, are measured in the centre of mass frame.

However, at higher energies the bell tends more to a plateau shape. The value of this plateau is approximately 2 charged particles. The explanation to the shape is that the particle production along the string (in figure 2.4.) is uniformly distributed. This is a consequence of the fact that the wounded quark is uniformly distributed between the rapidity of the two protons. A figure of this can be seen in *figure 2.6* where one of the protons rapidity has been set to zero.

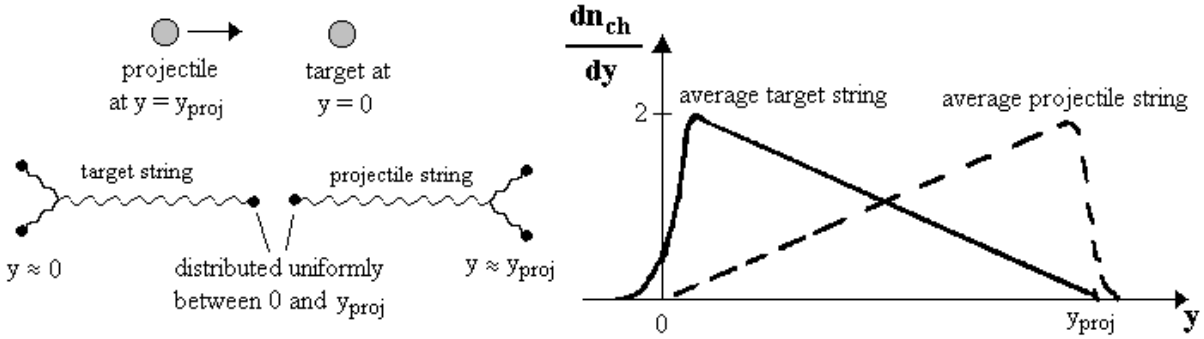

Figure 2.6: The left part of the figure shows how the wounded quarks are distributed and the right part shows how the multiplicity is distributed. From the right figure it is easy to understand that the sum of the two distribution curves will add up to a plateau.

Chapter 3.
- AA-Collisions

3.1 – Introduction

In the previous chapter we talked about proton-proton-collisions. A naive and straight forward assumption would be that the nucleus-nucleus-collision (AA-collision) would be a superposition of these. But this is not the case. In the AA-collision new phenomena called *collective effects* are observed. These collective effects can be found by comparing the pp-collisions with the AA-collisions. The differences should then be due to the fact that there are more nucleons involved in the reaction. This is the reason why it is very important to understand how the pp-collisions work. Basically the same quantities that are used in pp-collisions are used in AA-collisions. However, the number of particles produced in the AA-collisions is many orders larger and the data is thus harder to analyze.

3.2 – From PP to AA- Collisions

In the step between electron and positron collisions we go from points to something with at least some kind of extension. The way a collision can behave then goes from the two options, hit or miss, to more complicated situations such as some kind of overlap region. In the further step, to nuclei collisions, it becomes even more complicated. Therefore a parameter which describes the reaction was developed, the *impact parameter* denoted b (*figure 3.1*). If the two nuclei hit each other as central as possibly the value of be is 0. And if the barley hit each other the value is slightly less than R_A+R_B, where R_A and R_B are the radii of the two nuclei.

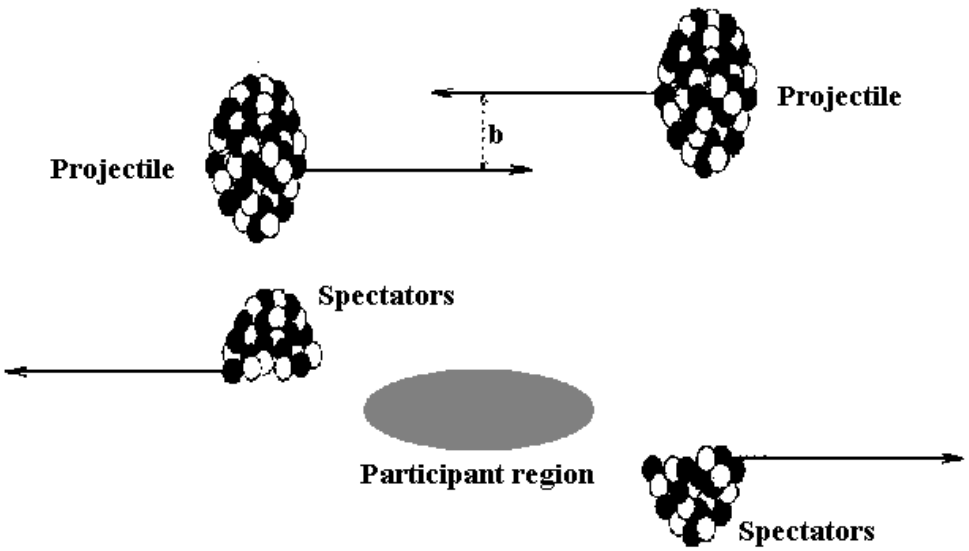

Figure 3.1: In the upper figure the impact parameter is shown as the distance between the centres of the colliding nuclei. The lower figure shows how the spectator nucleons just continuous on their path, while the participating nucleons form a highly energetic soup.

It is very unusual that a collision occur in a way so that all the nucleons participate, but this is not only dependent on b. Another thing affecting the number of participating nucleons is the size on the ions. Think e.g. on a collision between a proton and a led nuclei. In this example a

lot of the led nucleons would of course never participate in the collision, even if the value of b was 0. The nucleons that participate in the collisions are called *participants*, while the other nucleons are called *spectators*, drawn in *figure 3.1*. An interesting thing about the spectators is that they do not notice when the collision occur. So while the participants form a highly energetic nuclei soup, the spectators just continue on their path. In many cases the spectators form unstable nuclei which rapidly decay. The interesting physics (for this specific topic) is the physics in the *participating region*, the region made up by the participants. So from now on we will just discuss this region.

One key feature to understand how the AA-collisions work, from the view of PP-collisions, is to understand how the nucleons interact. The actual collision process is hard to simulate, so instead approximation methods are used. One such method is the *binary collision method* [6]. In this method a collision between e.g. a proton and a nucleus is divided into several collisions. In each of these collisions the proton collides with each of the *relevant nucleons* in the nuclei. What is meant by the relevant nucleons can be seen in *figure 3.2*. It is simply the

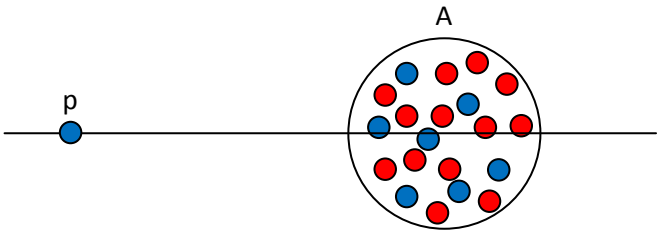

Figure 3.2: Here the proton beam is indicated by the line. Since the line crosses 4 nucleons in the nuclei, there will be 4 binary collisions.

nucleons which lie approximately in the beam direction of the proton and may interact with it. At every such interaction, a new path for the proton is calculated, to at last get an approximation for the whole collision. In reality the proton may bend of a bit after the interactions, but to understand the principles it is enough to think of a straight line. So if the proton is about to collide with a nucleus with 4 relevant nucleons, there will be 4 binary collisions. If instead the proton is another nuclei with four relevant nucleons there will be up to 16 binary collisions (if all the nucleons collide with each other).
In more advanced approximations it is possible to incorporate the other nucleons in phenomena such as rescattering.

With the number of binary collisions defined, it is possible to define the *nuclear modification factor* [7]. This quantity measure the deviation in yield between an AB-collision relative a scaled proton-proton yield. It is defined via:

$$R_{AB} = \frac{N_{AB}}{N_{PP} < N_{bin} >}$$

Here N_{AB} is the yield in a collision between nuclei A and B, N_{PP} the yield in a proton-proton-collision and $<N_{bin}>$ the mean of binary collisions in the A-B-collisions. To investigate the behaviour of the collisions, it is often customary to choose nuclei A and B to be different

spices. It is e.g. of great importance to investigate the modification factor when either A or B is a very light nuclei or even a proton. From experiments such as these, it is possible to find phenomena that occur independently of the collided nuclei. One such example is *shadowing* [8], which is a phenomenon where the structure functions for the nucleons are deformed. This causes the particle productions in the collisions to change. Another phenomenon affecting the particle yield is *gluon saturation*. This phenomenon is caused when the gluons in the hadron form a new state, the so called *color glass condensate* (CGC). Both shadowing and gluon saturation is far to advanced for this thesis, thus the interested reader should look up the references.

From the theory above, it is possibly to extract some of the collective effects out of the AA-collisions.

Chapter 4.
- QGP (Quark-Gluon-Plasma)

4.1 - Introduction

Early in our physics education we learn about different states of aggregation. The first three we learn about is the solid, the fluid and the gas states, the three everyday encountered states. If we go to energies higher than in these states we eventually learn about a state we call plasma. In principle this state is not anything strange or exotic, which maybe the name may imply, but is rather the most common form of matter in the universe. In this state the particles have energy high enough to break the Coulomb force between them. This result in a matter where the charged particles can move around freely and are not combined to molecules or atoms. Examples of where this kind of matter can be found are in stars and fires. The criteria to create plasma are either a very high temperature or a very high density. If the temperature or density is passed far beyond this limit we expect at some point to find a new *phase transition* into an even more energetic state, the so called Quark-Gluon-Plasma. This state of matter can be created through collisions between nuclei at extremely high velocities.

4.2 – The States of Strongly Interacting Matter

As stated in the introduction there must be some kind of phase transition for nuclear matter to become a QGP. This transition is dependent on both the temperature and the density (and some other parameters as well) of the matter. Usually some other quantities like *chemical potentials for baryons* (μ_b) or something similar is used instead of density, but serves the same purpose. If fact μ_b is a quantity describing how many baryons there are in relation to ant-baryons. In *figure 4.1* a phase diagram for nuclear matter is shown where the parameters are temperature and the chemical potential. From this we can get some insight in how we can change the parameters to create different states of the strongly interacting matter.

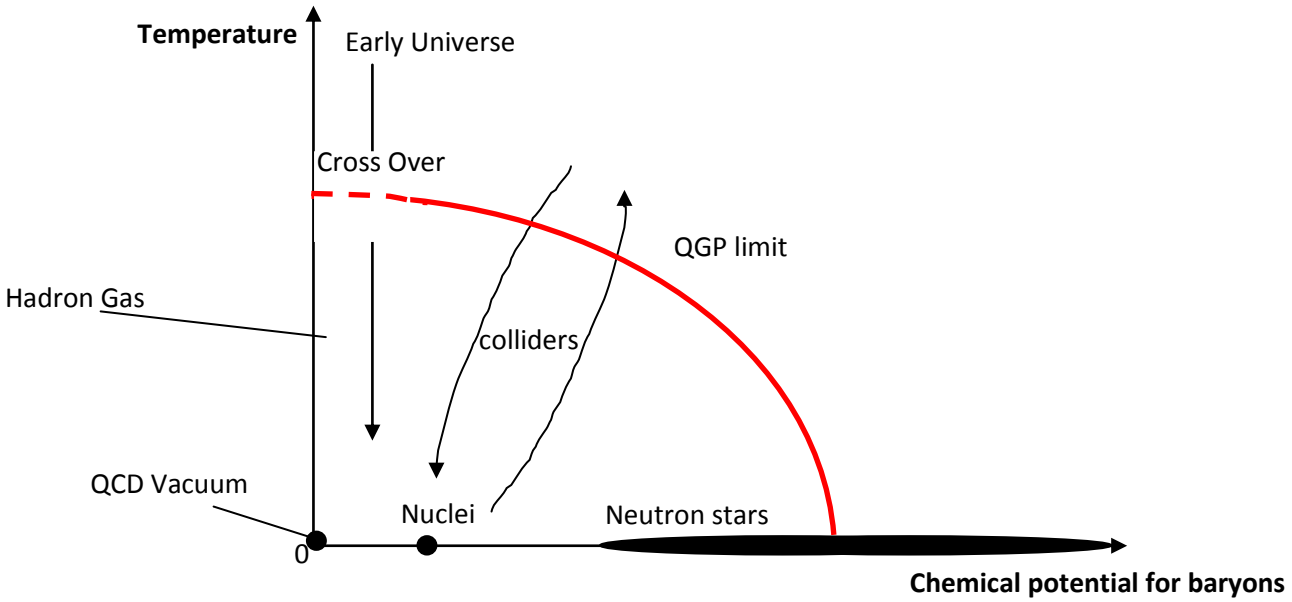

Figure 4.1: A phase transition diagram for nuclear matter.

If we begin in the lower left corner of the diagram we have very small values on both the parameters. This region is often referred to as the *QCD- vacuum*. It is in this low energy region it is adequate to use QCD instead of *perturbation-QCD* [4]. Thus this is the region which was described in chapter 1. If we move a bit to the left of this point, or in other words increase the chemical potential, we find "normal" nuclear matter. If the temperature is left unchanged and the chemical potential is increased by somewhere between 2-10 times compared to nuclei, we enter the region of neutron stars. In certain parts of this region it is possible for QGP to exist. This QGP region also extends in a curve from the neutron stars on the chemical potential axis to higher temperatures on the temperature axis. The matter in the core (the area bounded by the axes and the curve) is in a state which is called hadron gas. Outside this curve we have the state that traditionally is called QGP. If we try to reach this state by just changing the temperature we have to go through the *cross over* zone. In this zone the matter is believed to change from the hadron gas to the QGP in a rapid by continuously way and not in a classical phase transition. The temperature needed to achieve the QGP is calculated by lattice QCD to be around 170 MeV at small values of μ_b.
In the limit where we let the temperature go to values far above 170 MeV, while keeping the chemical potential fixed at low values, we at one point will end up in a state very much like the *early universe*. In the first fractions of seconds after Big-Bang the universe expanded incredibly rapid, this made it cooler. So at one point in time, the universe went through the transition from QGP down to the hadron gas, and the matter we know today. A little more on this topic and on neutron stars will be the subjects in *section 4.4*. [9]

In the experiments where the goal is to recreate the QGP, the current way to do so is through a combination of high temperature and high chemical potential. Even if the attempt to create it is successful, the time it will be present is very short. So all that is reasonable to hope for, is a quick visit in the QGP region before the matter cools off and become normal matter again.

4.3 - Possible Evidence of the QGP

The conditions to create a QGP are very hard to fulfill. The high energy and density needed will e.g. only be present a short period of time after the collisions. After this the QGP will return to a hadron gas. Therefore it is of great importance to know what kind of signals we are looking for as evidence for the QGP. There are several ideas of what could be interpreted as evidence. The ones discussed here are:

- Strangeness and charm Enhancement
- J/Ψ-suppression
- Jet-quenching and high P_t-suppression

All of these three phenomena have in one or another way been observed, which indicates that QGP actually have been created in collisions. But for some of them it has recently been questioned whether they really have been observed or if the data have been interpreted in an incorrect way. How the experiments are preformed is discussed in *Chapter 5 – The*

[4] At high energies perturbation theory is used to derive pQCD. For further reading see e.g. *Basics of Perturbative QCD* by Yu. L. Dokshitzer et al.

Experiments and the Equipment. In the section after that, *Chapter 6 – Results*, a discussion of how the above listed evidences have been interpreted. In this section we will also see phenomena that from the beginning not were expected, but later proved to be hot topics to deduce whether or not a QGP have been created.

Before we try to understand the signals from a QGP we should try to understand which proporties we expect it to have. To do so it is appropiate to think of two nuclei collide at ultra-relativistic speed. Let us assume that the collision occurs with a small impact parameter, b, so that a relatively large region of participating nucleons is created. The high kinetic energy in this region then squeeze the nucleons together in such a way that they overlap. Due to this the quarks no longer know to which nucleon they belong and start to move freely inside the overlap region (known as the QGP), see *figure 4.2*. So some important properties that can be expected from this are:

- The QGP is a system made up of quarks and gluons rather than several independent nucleons.
- The free partons in the QGP create a coloured field.

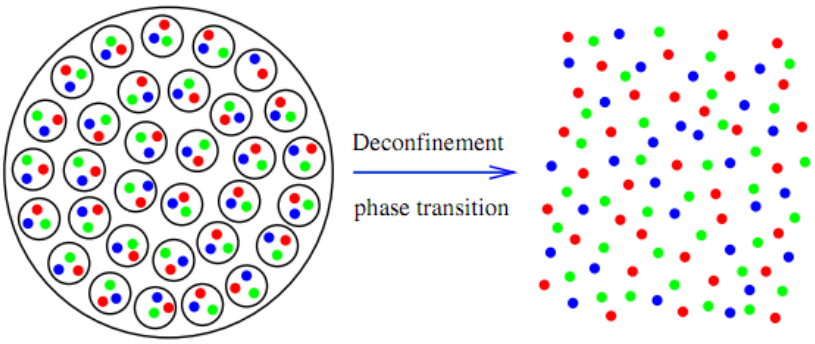

Figure 4.2: The left picture shows the nuclei in the moment precisely before they collide. The right figure shows the situation shortly afterwards. Here the quarks are deconfined in the QGP-region.

It might also be of interest to point out that the theorists thought of the QGP as a weakly interacting gas before any experimental data pointed in another direction. However this changed after some results, that we will come to in a later chapter, and QGP is today commonly accepted to be more of a fluid with low viscosity. But with higher energies it is possible to explore new phenomena. It might be that there is a limit where the QGP turns into a gas.

4.3.1 – Strangeness and Charm Enhancement

In the high energetic QGP all the quarks is combined to one system. A consequence of this is that they have to obey the Pauli Exclusion Principle. To do so the up and down quarks (the most common quarks in the hadrons) have to occupy quantum states with very high energies. At some point this energy is so high that it is energetically preferable to create heaver quarks instead of exciting the lighter. As can be seen from *Table 1-1*the second generation quarks are the lightest after the up and down quarks. So these are the ones one expects to be produced in a collision where a QGP is created. Since the s-quark only have a mass, roughly 1/10:th of the c-quarks mass, it is also natural to expect the major part of the created quarks to be s-quarks. However, the signal physicists are looking for when it comes to s/c enhancement is an

increased amount of strange or charmed hadrons. If one calculated the number of e.g. hyperons (particles with s-quarks) per non-hyperons as a function of energy density one would at one point see a rise in the curve. This is the *critical energy density* (ε_c), which is the energy density to have the phase transition to QGP. A graph of this can be seen in *figure 4.3*.

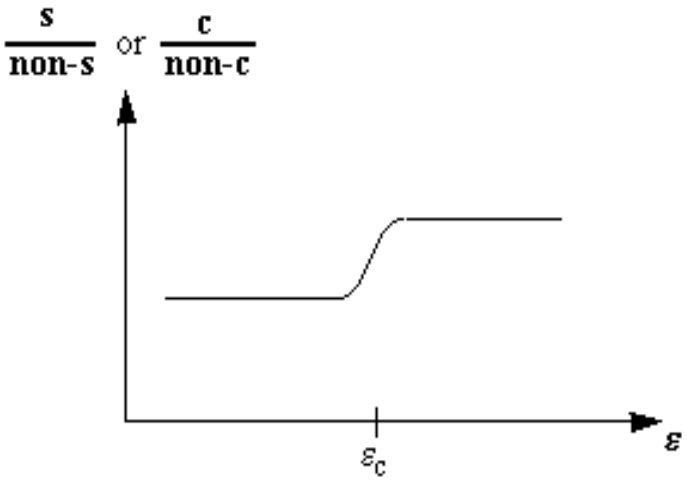

Figure 4.3: Here is a graph showing the fraction of charmed particles per non-charmed versus energy density.

4.3.2 - J/Ψ-suppression

In the previous section we concluded that it seems reasonable to think that more c-quarks (or rather charmed particles) will be detected if a QGP is present. A special meson made up by the c and $\bar{c}$-quark is the *charmonium*. Its ground state it is denoted by J/Ψ and its first excited state by Ψ'. At first one may think that we will detect more of these charmonium states, since there will be more c-quarks produced. But in fact it is the opposite we expect to see, and this is called *J/Ψ-suppression* or more general charmonium-suppression. The reason for this is that the produced $c/\bar{c}$-quarks in a normal matter would be more likely to combine with each other. This since there is no or at least few other free quarks to combine with. But in a QGP there are lots of other free quarks to combine with instead. So when the energy density rise the amount of charmonia detected is expected go down. The dissociation energy for the J/Ψ is around $2.1T_c$, where T_c is the critical temperature for a QGP. The same dissociation energy for the exited state is expected to be much lower, at $1.1\text{-}1.2T_c$. These calculations are done with lattice QCD.

The same suppression process is also expected to another *quarkonia*, coupled quark-anti-quark pair, namely the $b\bar{b}$ denoted Υ. This particle is of course much heavier than any of the above charmonium states, but the principle of suppression should be the same anyhow.

4.3.3 - Jet-quenching and High P_t-suppression

In the collisions between two nuclei there is a certain probability for jet events. In section 1.4 we learnt that the jets are due to hadronization of coloured particles. The idea here is that these coloured quarks have to travel through the coloured QGP before we can detect the particles they fragment into. So on its way the particles will interact strongly with several other coloured partons and loose energy. This is called *gluon-bremsstrahlung* since the

interaction is mediated by the emitted gluons from the particle. This is a similar phenomenon to the bremsstrahlung, which is when a charged particle emits photons when it travels in an inhomogeneous electric field.
Let us e.g. consider a two jet event. Since the origins of the jets are more or less arbitrary one specific origin could be near the edge of the QGP. Then one of the two particles that will fragment must travel a much longer way through the QGP. Thus it would lose energy and the hadrons produced in this jet would have a lower energy in comparison to the other jet (See *figure 4.4*). This is to say that the jet has been quenched. In an experiment the result would be one strong jet and a much weaker jet in the opposite direction to the first one. Of course is it probably so that the weaker jet will contain more particles. But since these particles have lower energies, the software used is built in such a way that it will not count the particles if they do not have certain threshold energy. A schematic result of an experiment where jet-quenching has occurred can be seen in *figure 4.5*.

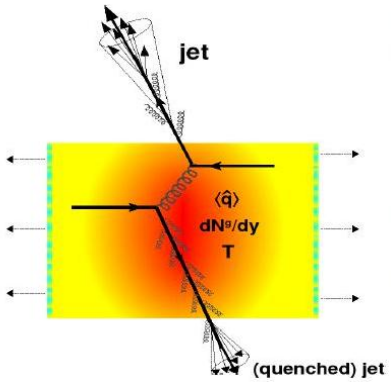

Figure 4.4: The upper jet is more or less unaffected while the lower is quenched in the QGP.

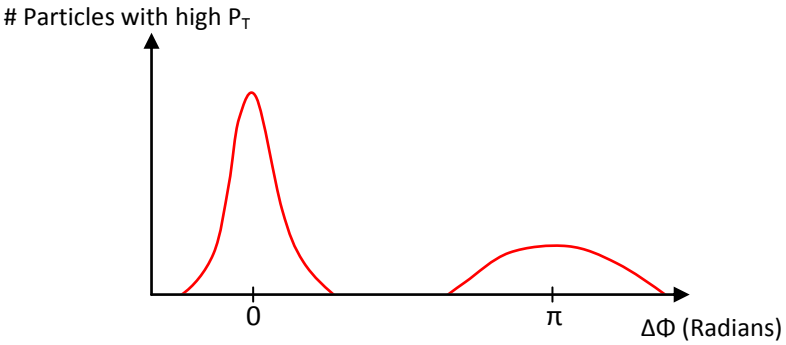

Figure 4.5: The left peak is the so called trigger jet. This is the un-quenched jet and thus this jet contains more particles with high transverse momentum than the right, which is the quneched jet.

A phenomena closely related to the jet-quenching is high hadron p_t-suppression. This suggests that if a QGP is produced in a collision, then fewer hadrons with high p_t should be observed. This is due to the fact that eventual jets will be quenched. Jet-quenching can only be observed if the jets are produced near the edge of the QGP. But to observe high p_t-suppression, this geometry is not needed.

4.4 – QGP not created by Human

There are at least two different places in universe, where we expect the QGP have been created. The first one is *early after Big-bang*, the birth of universe, and the second in *neutron stars*. These are two places in universe with either a temperature or density high enough to create this state of matter.

All the energy and material we know of today have one time, about10^{10} years ago [10], been focused in just one single point. This was in the earliest moment of the creation of the universe. Just a few fractions of seconds later, the energy in that point had expanded to a several kilometres wide fire ball. In this instant the temperature was billions of degrees high. So the extreme energies needed to create a QGP were without any doubt achieved here. So to

understand why the universe developed the way it did a key point is to understand how the QGP works. This is an interesting idea that connects high energy physics and astronomy, a connection between the smallest and largest scale in physics.

Also the neutron stars are subjects treated in astronomy. Even though the energy and density here is on a completely different scale they are still enormous. Hence it is a simplification to talk about these masses in terms of solar masses, $M_{\odot}$, which is about $2 \cdot 10^{30}$ kg. The limit where a star becomes a neutron star is approximately just above $1.4M_{\odot}$. If a mass like this is reached, the pressure in the star can no longer resist the gravitational force. Thus the star is compressed and its density is greatly increased until the star has found a new equilibrium. It is these stars in this equilibrium that referred to when spoken about neutron stars.
The diameter of these objects is usually of the range 10km (compare to the Sun with an over 100 000 longer diameter), so they are actually much smaller than Earth. The surface of the neutron stars consists mainly of metals creating a solid. Hence, on this distance from the stars midpoint there actually exist both electrons and protons to create atoms. In the surface the density is relatively low ($\sim 10^7$ kg/m^3), compared to the mantle and core of the star. Only a few km inside the star, in the mantle, the density rapidly increases several thousand times. Here almost all the matter is neutrons, which is in a superfluid state. Even deeper in the star, in the core, the density reaches a value of 10^{18} kg/m^3 and higher. It is here, in the core, we expect the QGP exist. [11]

So just like the researches, that try to understand the early Universe, the studies of neutron stars can complement the high energy experiments. The rotation of the stars in combination with their strongly magnetic fields makes it possible to observe data from them. These data could perhaps be used to explore the inner structure of the stars, the QGP.

Chapter 5.
- The Experiments and the Equipment

5.1 – Introduction

In the previous chapters we have mainly talked about the theories and the expectations we have. In this chapter we will move on and talk about the actual experiments that have been and will be preformed. The experiments are more or less concentrated to 2 facilities, RHIC at Brookhaven National Lab in the US and at LHC at CERN on the border between France and Switzerland. Both at RHIC and at LHC one aim is to detect and investigate the QGP. RHIC was taken in use a few years earlier than LCH (which currently is running below its maximum energy) and is designed in a somewhat different way. Thus it is easier to divide this chapter into one chapter concerning the experiments on RHIC and one concerning the experiments on LHC. But before that, some of the common features are to be established.

5.2 – The Accelerators

Not very surprisingly, both RHIC and LHC need to accelerate ions to perform the experiments. Producing these ions is one of the earliest stages in a long chain where the aim is to create a QGP. The most commonly used sources of ions are plasma-based [12]. From the plasma the ions are, by use of voltage gaps, extracted into a vacuum chamber. The ions are then accelerated in a *linear accelerator*, inside a *vacuum tube*, which accelerates the ions by varying an electromagnetic field [3]. The reason to keep the particles in a vacuum tube is to prevent them from interacting with the particles in the air. The electrical field is often produced by a voltage which oscillates as a sine curve. Due to this behaviour of the field, some of the ions are accelerated while others are decelerated. To prevent the decelerations from occur, the accelerators are built in a way so that *drift tubes* isolate the ions which else would have been decelerated. The drift tubes are built in a material which the electromagnetic field cannot penetrate. So in these, the ions are at rest, while being accelerated outside of them, see *figure 5.1*.

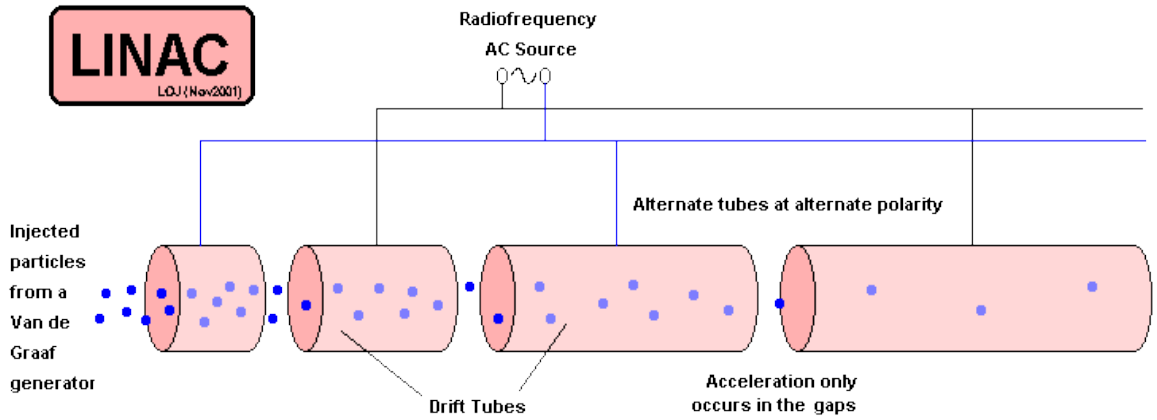

Figure 5.1: Here the drift tubes shields the particles when the field is decelerating them. In this case the particle source is a Van de Graaf generator. Instead of changing the length of the drift tubes, it is possible gradually change the alternating field as the particles gain a higher speed.

As the velocity of the ions is increased, either the length of the drift tube or the frequency of the electromagnetic field must change.

After the ions have passed the linear accelerator they are ejected into the *synchrotrons*. These accelerators are formed as rings, so that the ions can be accelerated several times in the same machine. Since the path is not straight, the ion beam have to be bent, this is achieved using strong magnetic fields, applied perpendicular to the bending plane. To keep the ion beam in position as the momentum increases, the magnetic field is increased as well. So the name of the synchrotrons comes from the fact that the electric and magnetic field are synchronized. The acceleration in the synchrotrons is also due to alternating electromagnetic fields, just like for the linear accelerators.

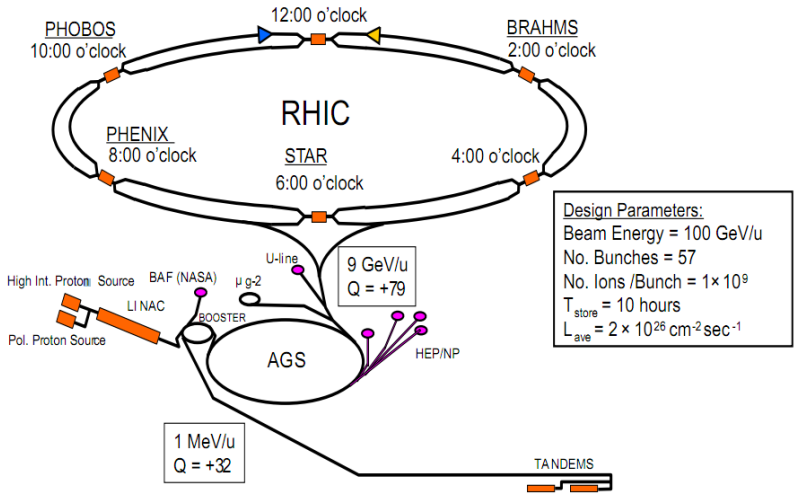

Figure 5.2: RHIC

In *figure 5.2* the RHIC accelerator is shown, together with some additional information. RHIC can accelerate both heavy ions and protons. If ions are accelerated, they are taken from the Tandem Van de Graaf generator. When they are taken from here, they always have several electrons left which must be taken care of by various means. If it instead is protons that are accelerated, then they are taken from the proton source. Both the ions and the protons are taken from their sources in *bunches*, i.e. lots of particles are accelerated together instead of particles being accelerated one by one. In both cases they are first accelerated in a linear accelerator which leads them to the first synchrotron, the booster. In the booster they have their velocities greatly increased before they are injected into the AGS (Alternating Gradient Synchrotron). In between the steps when the ions are injected into another accelerator they are going through a foil where the electrons are torn off. Well in the AGS, the bunches are accelerated to a speed only a few parts of a percent from the speed of light. From here it is possible send the particles to either a fixed target experiment or to RHIC (we will only follow the path leading to RHIC). When the bunches are ejected out from the AGS they follow a pipe leading to RHIC. In the end of this pipe there is a road junction. Half of the bunches are guided by magnets in one of the directions and the other bunches in the other. From here on they will be accelerated in opposite direction in separated tubes. At certain points these tubes

crosses, so that the particle beams can collide there. It is at these points the detectors are stationed.

Some of the benefits of a synchrotron are that even though not all the particles in the bunches collides, they will not be lost (like they would in a fixed target experiment). Instead they continue to travel in the beam tube and may collide at some other point. Thus these kinds of accelerators can keep on colliding particles for several hours before they need new bunches. This is of course a very energy-saving way to perform highly energetic particle collisions. Another benefit is that the available energy in the collision is much higher for this kind of collisions compared to fixed target.

Unfortunately there are some complications when it comes to synchrotrons. For example is energy lost when the bunches are bended to follow the circular path. This is however good for facilities which uses synchrotron radiation, but not good in e.g. heavy ion collision experiments. The synchrotron radiation emitted is inversely proportional to the bending radius. Thus it can be suppressed if the radius is very large, but at some point it is not feasible to build larger accelerators.

5.3 – The Detectors

As we learnt in the first chapter, there are several kinds of particles, all with their special properties. Some particles are electrically neutral and light, while others are electrically charged and heavy. All these kinds of differences can be used to our advantage when we want to determine which kinds of particles we have produced in our experiments. But to do so, it is necessary to measure with many different detectors. In high energy physics, the collision points are covered in several layers of detectors. Some of them measure photons while other measure electrons etc. An introduction to the detectors will be given here in this section. First we discuss the *gas detectors*, which are detectors that can be used to detect the particles trajectories. The next groups of detectors are among other things used to detect charged particles and measure their velocities. These groups are the *solid-state detectors*, the *scintillator detectors* and the *Čerenkov detector*. At last we have the detectors that measure the total energy of the detected particle, both charged and uncharged. These are called *calorimeters*.
The last part of section 5.3 will briefly discuss how the detectors are put together to work as efficiently as possible.

5.3.1 – Gas Detectors

One of the simplest examples of a gas detector is a Geiger counter [2] [3]. This is a gas filled tube with an anode wire in the middle and cathode as wall, see *figure 5.3*.

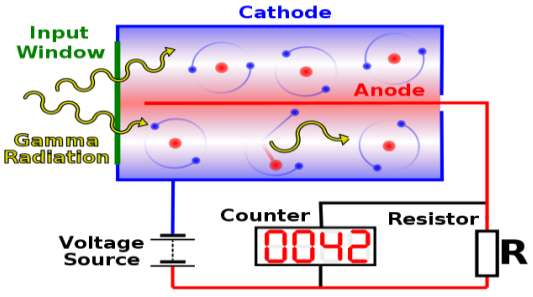

Figure 5.3: A schematic picture of how a Geiger counter is constructed.

The voltage between the anode and cathode is usually large, of the order hundred of volts. When a particle traverses the gas, it also ionizes it along its path. Since the electrons and ions are in a strong field, they are accelerated against the anode or the cathode respectively. In this acceleration they often reach such a high velocity, that they themselves ionize the gas. Thus it is finally a whole cascade of ions that reaches the anode. This creates an output signal at the anode and thus we know that a particle just traversed our detector.

If it was possible to build a construction with a lot of Geiger counters in a larger volume, it would be possible to follow a particles trajectory. This is however not effective, nor used. Instead larger cathode plates are used to build the *multiwire proportional chambers* (MWPT). In these plates are the anode wires incorporated. This is shown in *figure 5.4*. Each of the anodes has their own output channel, which makes it possible to decide one of the two coordinates in the cathode plane. If every second plate is rotated so that the wires of the upper plane are orthogonal to those of the lower plane, the second coordinate can be decided as well. The accuracy of this coordinate is dependent on the spacing between the anode wires.

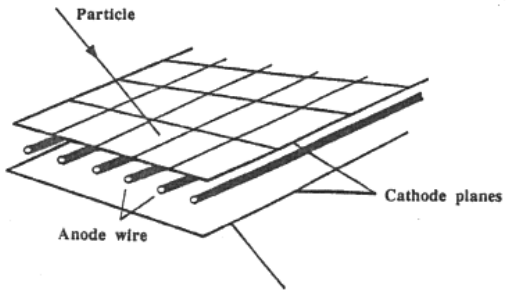

Figure 5.4: Here the cathodes are plates rather than a cylindrical shell. If another plane is put on top of this, but rotated 90˚, it is possible to decide the coordinate in the plane where the particle traverses the plane.

The step from the Geiger counter to the MWPT was a great improvement. The MWPT can detect particles up to a resolution around 50μm in about 2ns. However, it is today rarely used. Instead a *drift chamber* is used. This detector uses the fact that is takes some time for the ions to *drift* from the creation point to the anode. If the drift velocity for the gas at the certain voltage is known, it is possible to construct the particles trajectory. To do this, it is however necessary to use trigger detector (see scintillator detectors below) to measure time differences between two events. The two figures 1.7 and 1.8, displaying jets, are produced with drift chambers.
One disadvantage of the MWPT is the problems encountered when several particles are tracked in the device. If the particles traverse the MWPT in a small area, it is very hard to decide which signal that belongs to which particle. So in heavy ion collisions, where many particles are produced, it is almost impossible to combine the information given in the different layers. However, the accuracy can be improved by incorporating even more wires in a new geometric pattern.

One application of the previous described detectors is the *time projection chamber* (TPC). This is a barrel-shaped detector, usually a few meters long and about one or two meter in diameter. The beam pipe goes through the middle of the barrel, which is filled with a gas. At the flat ends of the barrel, there are layers of MWPTs. Due to two electric fields, pointing inwards from the middle of the barrel (see *figure 5.5*), the created electrons are accelerated towards the MWPT. Here they are measured to create a two dimensional (in the plane

orthogonal to the beam pipe) trajectory after the ionization particle. To get the third coordinate, the same ideas as for the drift chamber are used. Namely that it takes a certain time for the particles to drift before the hit the anode.
If the TPC is placed in a strong magnetic field it is possible to determine the momentum of the particle. This is done by investigating the curvature of the trajectory (in the case for a charged particle).

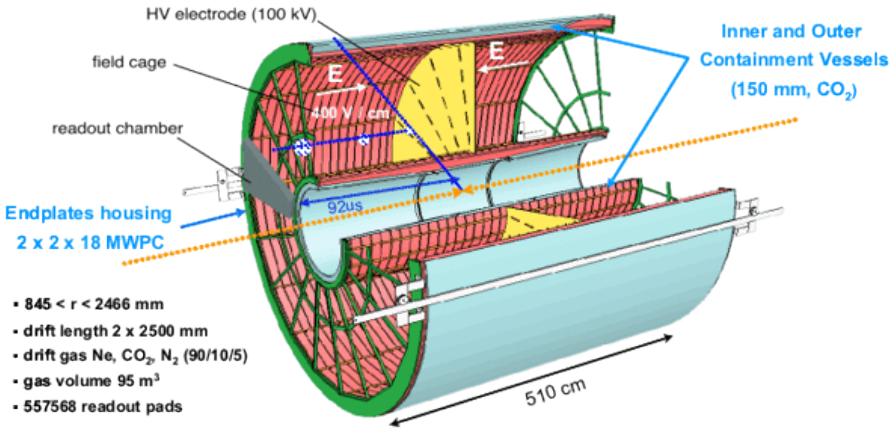

Figure 5.5: A TPC used in the ALICE-experiment.

Beside the above described abilities of the TPC it can also measure the ionization, or the energy loss, in the gas. This quantity can, if it is measured in several points together with the particles momentum, serve as a measurement of the particles mass. To measure the ionization per unit length, dE/dx, the liberated electrons in the particles trajectory is measured. Thus it is important to not have too high voltage between the poles in the TPC. If the voltage is too high, then the electron pulse will not be proportional to the number actual liberated electrons (the electrons would create a cascade, compare to the Geiger-Counters). The mass of the particle can be deduced by use of the *Bete-Bloch-formula* [3]:

$$-\frac{dE}{dx} = \frac{4\pi}{m_e c^2} \cdot \frac{nz^2}{\beta^2} \cdot \frac{e^2}{4\pi\varepsilon_0} \left[\ln\left(\frac{2m_e c^2 \beta^2}{I(1-\beta^2)}\right) - \beta^2\right]$$

Here n is the density of atomic electrons and I the average atomic excitation potential. The Bete-Bloch-formula can plotted as a function of velocity (β). As the velocity increases, the function decreases, due to the $1/\beta^2$ dependence. This continues until the function reaches a minimum, the minimum ionization region. It is in this region that the particles are easiest to distinguish from each other. After the minimum the function increases until it reaches a constant value. Some experimental data showing dE/dx plotted versus momentum can be seen in *figure 5.6*.

An even newer invention is the *microstrip gas chamber* (MSGC). It is in many aspects similar to the TPC, but uses a plate of conducting metal instead of the wires in the MWPC.

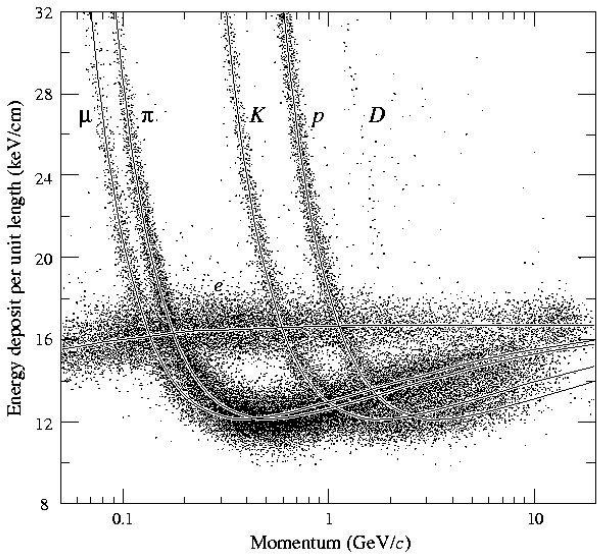

Figure 5.6: In these measurements the particle types have been decided by comparing the data to the Bete-Bloch-formula.

5.3.2 – Semiconductor detectors

The idea behind the semiconductor detectors is to use the *band gap* (BG) in solids, which for semiconductors is the region between the *valence band* (VB) and the *conducting band* (CB). The VB is the highest energy level an electron in the solid can occupy, while the CB is the energy level above the VB. The energy gap between these two levels is called the BG, see *figure 5.7*.

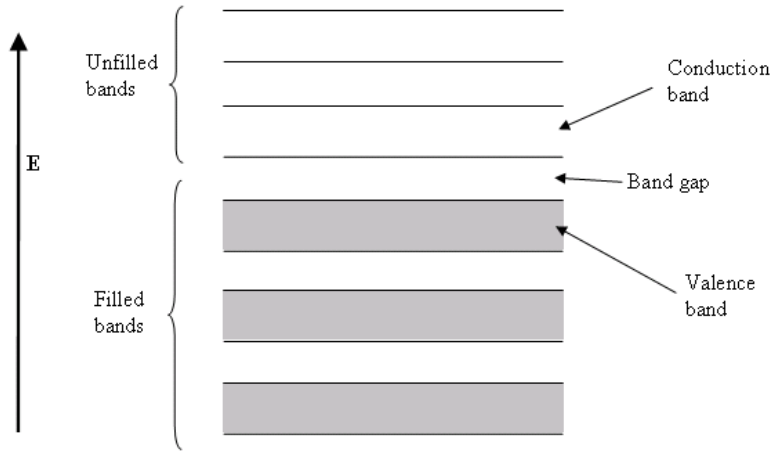

Figure 5.7: The band structure in a solid. For conductors, the VB and CB overlap (no BG), and not all electrons are used to create bonds between atoms. Thus the electrons can move freely, giving rise to good conductivity. For insulators it is the opposite way. They have large BGs and conduct therefore poorly. The semiconductors are in between these two materials.

To make the detectors work efficient, one creates a so called *pn-junction*. This is achieved by adding an *n-doped* material with a *p-doped*. An n-doped material is a material with an abundance of electrons. This can be obtained by substituting some of the original atoms in the material with atoms with more electrons. If this is done one gets a material where electrons lie just below the CB and can easily be excited up to it. The same is true for p-doping, but in the opposite way, which means that the holes lie just above the valence band VB. If the n-doped material is put together with the p-doped, there will be an area between them where the electrons and the holes cancel each other. This is called the depletion region (DR) and is a

region without any charge carriers. But the doped materials are still charged and create thus an electrical field through the DR. It is this area of the material that works as our detector, and to make this region larger a reverse bias is applied over the material. So when a charged particle traverses the detector, it creates electron-hole pairs. This is done in a way so that the number of pair produced is proportional to the energy of the particle. Since both the electrons and the holes are charged, they will drift to either the p-doped or n-doped side where they will be detected as charge pulses. A picture of this can be seen in *figure 5.8*.

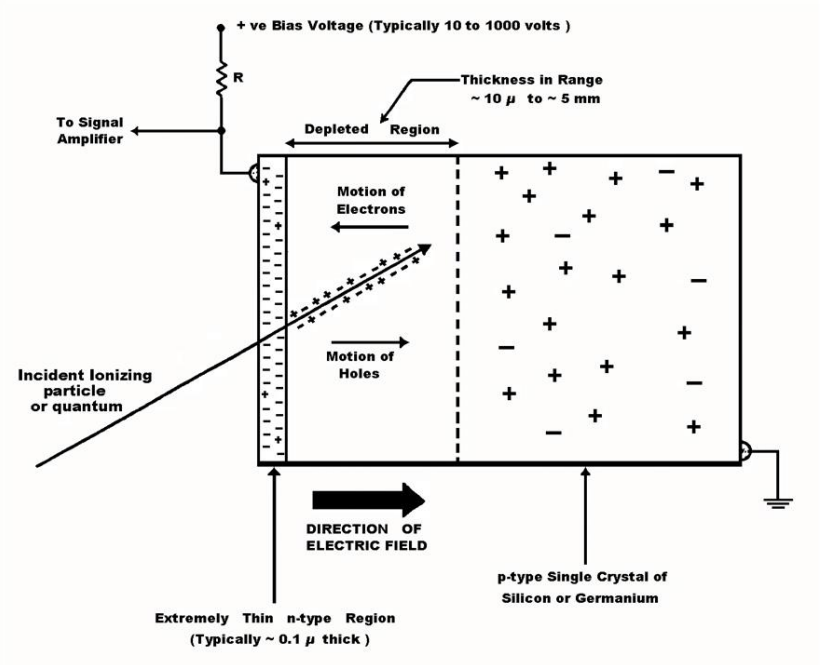

Figure 5.8: When a particle enters the DR it creates electrons and holes. These can be measured to determine the traversing particles energy.

One advantage for the semiconductor detector compared to the gas detectors is that is uses holes and electrons instead of electrons and ions. Thus less energy is needed to create a signal in the detector. This makes it more accurate and it is able to detect particles with energy as low as just a few eV.
The detectors are many times placed near the collision points in experiments to detect particles from the decay of short-lived particles. In this case it is often a type of detector that is called *silicon microstrip detector*.

5.3.3 – Scintillator detectors

Another frequently used detector is the *scintillator detector*. A scintillator detector consists more or less of one scintillator part and one photo multiplier tube (PMT) part. When a charged particle passes through the scintillator, the atoms in the scintillator become excited. When the atoms later decay into their ground state, they radiate photons which are collected by a light-guide. This device guides the photons to the PMT. When the photons come to the PMT they hit a photo cathode. Here they are absorbed, while a few electrons are realised. These electrons are then multiplied, by multiple accelerations against anodes. In the final step a charge pulse can be read of the PMT. It should be mentioned that the number of radiated

photons from the scintillator is proportional to the charge pulse given by the PMT [13]. The process is illustrated in *figure 5.9*.

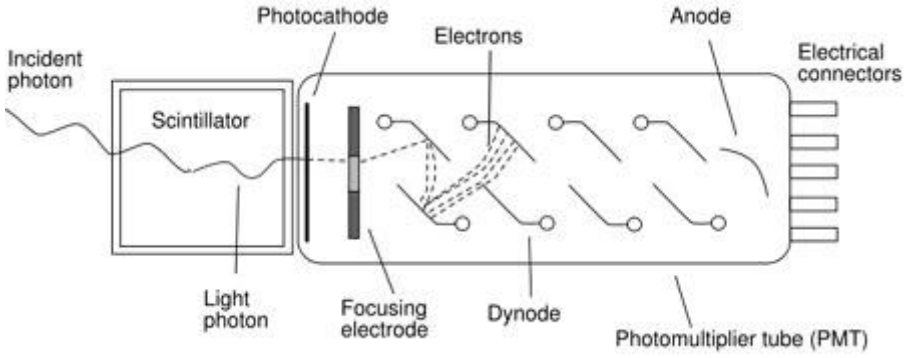

Figure 5.9: The idea of a scintillator detector.

The good time resolution of the scintillator detectors (100 ps) make them useful in a variety of detection methods. They are e.g. used for 'trigging' other detectors, which means that they, based on their measurements, decide whether another detector should measure or not. For particles with lower velocities they can also be used to measure the time-of-flight, which can be used to calculate a particles velocity. From this, together with the measurement of the objects momentum, it is possible to determine which kind of particle it was [2].

5.3.4 – Čerenkov Detectors

To explain how a Čerenkov detector (CD) works, it is necessary to know what the Čerenkov effect is. This is a phenomenon that occurs when a charged particle travels faster than light in a medium [2]. When the particle does so, it excites atoms along its trajectory and when these atoms de-excites, coherent radiation is emitted in an angle θ from the direction of the velocity. This is a phenomenon similar to a sonic boom, which is when an object travels faster than the sound. The angle the radiation is emitted in can be found from optical formulas (Huygen's principle) to be

$$cos\theta = \frac{1}{\beta n}.$$

Here β is the velocity of the particle divided by the light velocity and n is the refractive index of the material being traversed. This implies that it is possible to determine the particles velocity if the angle is measured and the refractive index is known. This is the idea behind the CD.

The CD has two major applications, as a threshold counter and in a ring-image detector. The first application uses the fact that the particle traversing the detector needs a certain velocity for the Čerenkov effect to occur. So with a Čerenkov detector it is possible to distinguish between highly relativistic particles in a sophisticated way. By changing the material in the detector, that is changing n, it is possible to get different threshold velocities.
The other application is a sphere-like detector. It consists of a photon detector inside a large spherical mirror. Between the detector and the mirror there is some kind of gas, in which Čerenkov radiation can be emitted. When a particle with high velocity go through the gas, the

Čerenkov light produced by it is reflected by the mirror down on the detector as a ring-image, illustrated in *figure 5.10*. The radius of the image is proportional to the angle θ, and it is hence possible to calculate the particles velocity.

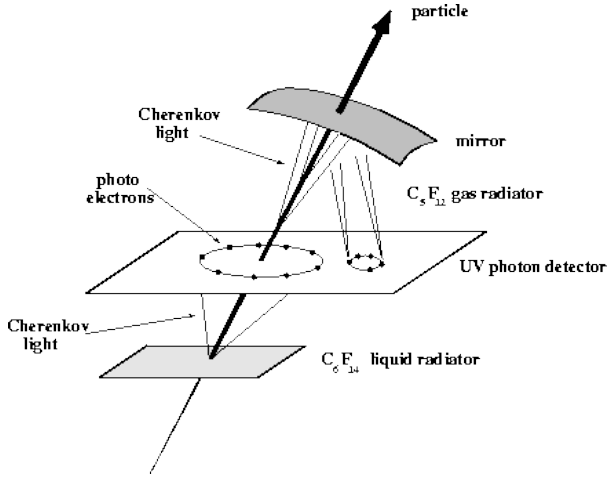

Figure 5.10: In this figure there is another Čerenkov medium before the particle goes through the detector. As can be seen, a ring-image is projected onto the detector by the mirror.

5.3.5 – Calorimeters

All the detectors discussed above have at least one thing in common; they do not absorb the particle. This is done in the calorimeters and gives the opportunity to measure both the particles energy and position.

The calorimeters can be constructed in several different ways. They can e.g. be made of scintillators or liquid argon combined in various ways. The construction used depends on which kinds of particles are being measured. There a roughly two main calorimeters; one electromagnetic and one hadronic. The electromagnetic calorimeter can measure electrons, positrons and photons, while the hadronic can measure hadrons. The idea for both types is the same; to have the particles interact with the material of the calorimeter so that *secondary particles* are produced. The ideal way of doing this would be so that all the energy of the particle is used up. The measurement of the secondary particles would then be a measurement of the particles initial energy.

For the electromagnetic calorimeters it is important to choose a material in which the particles are likely to interact via bremsstrahlung or undergo pair-production (bremsstrahlung for the electron and positron and pair-production for the photon). When the secondary particles have been produced, the initial particle will have a lower energy, this is illustrated if *figure 5.11*. By creating several other secondary particles along its trajectory, it might lose all its energy. Some of the secondary particles might get energy high enough to create secondary particles itself in a similar way. The total energy of the initial particle can then be calculated by counting the number of secondary particles produced.

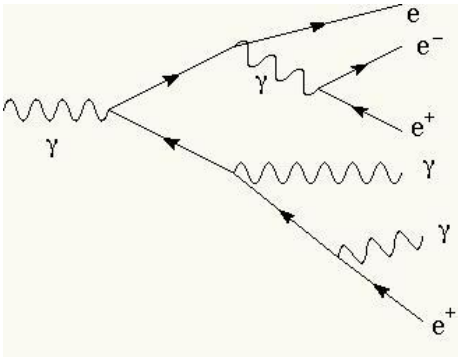

Figure 5.11: The initial particle in this case is a photon. After a certain length travelled in the calorimeter, the photon undergoes pair-production. This is the beginning of the electromagnetic shower that will come.

The hadronic calorimeters work in principle in the same way. But as one may expect, the absorption process here is more complicated. For example, processes involving muons and neutrinos can more frequently occur here. These particles are hard to detect, which results in a less accurate measurement of the hadrons energy. The length a hadron has to travel in a calorimeter before it produces secondary particles is also longer than for e.g. an electron. Thus the hadronic calorimeters are larger than the electromagnetic.

5.3.6 – How to Identify Particles

To identify particles and estimate their energies it is important to combine the different detector types in an efficient way. As we will see in section 5.4, then experiments are not designed in exactly the same manner. So what is efficient is sometimes a matter of which particles are supposed to be detected. For example is the ALICE detector at CERN designed to detect as many particles as possible and still give a high energy resolution and good trajectories. This may sounds like the ultimate particle detector, but one disadvantage is that it takes long time to collect all data. Specifically is the TPC a slow detector due to the long distances the electrons must travel before they can be collected at the anode. This long time to collect data is sometimes so limiting of an experiment that a TPC cannot be used. If we e.g. are searching for a very rare phenomenon which maybe only occurs a few times a day, we like to have a very short time between the collisions to collect as much data as possible. An example of this is the ATLAS detector at CERN, where no TPC is used. This is due to the rare occurrence of the production of Higgs particles, which ATLAS is searching for. Thus ATLAS is designed to collect and analyse data in a very small amount of time.
Although the experiments are constructed in their specific abilities, many of them have an underlying idea that is the same. Thus we will here, in a general way, discuss how the detectors are combined.

In *figure 5.12* we have a cross section of a high energy particle detector. Closest to the beam pipe (but no shown in the figure) is the vertex detectors. They are detectors with high position resolution, and are used to detect decay of short lived particles, mostly heavy baryons. If one can see the decay of a particle here, it is easier to find its corresponding decay-particles in the other detectors. The next detector layer is the TPC (light blue in the figure). From this both the particles

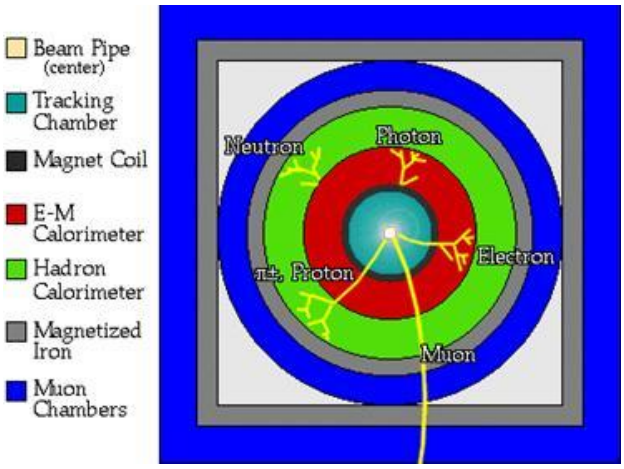

Figure 5.12: Cross section of a particle detector.

trajectories and dE/dx are measured. After the TPC is often a layer of TOF-detector (Time Of Fight) placed. These measures the time it takes for one particle to travel from one detector to another. In this way a velocity of the particle can be calculated. Note that these first layers do not absorb the particles, so they basically have the same energy as they had from the beginning. The absorption of the particles begins first in the next layers, in the calorimeters. The outermost of these detectors are the EM-calorimeters (red) followed by the hardron-calorimeters. They are used to measure the energy of the particles, as described in the previous section. But not all particles can be stopped in these detectors. Both neutrinos and muon can fairly easily traverse all of the detectors. Thus a layer of muon-calorimeters can be placed outside the other detectors, to at least detect some of the muons. The neutrinos are however too hard to stop.

5.4 – PHENIX and STAR at RHIC

The development of the PHENIX (the Pioneering High Energy Nuclear Interaction eXperiment) and the STAR (Solenoidal Tracker At RHIC) experiments started in 1991. About 9 years later, in year 2000, they and RHIC were completed and they were ready to collect data [14]. Back then, RHIC was the highest energy heavy-ion collider in the world and many fundamental properties were expected to be found and clarified in the experiment. Both PHENIX and STAR are thus designed to detect some of the possible signals a QGP will give rise to. PHENIX is e.g. specialized to detect the signals one could expect will occur in the phase transitions when the states of the hadronic matter are changed. This detector is therefore particularly good to detect photons and leptons from such transition. STAR on the hand is designed to efficiently investigate collisions by tracking the particles produced in the collisions. The energy range of RHIC is up $\sqrt{s_{NN}}$=200GeV for Au-Au-collisions and $\sqrt{s}$=500GeV for pp-collisions. This is thus the energies which PHENIX and STAR operates in. RHIC is shown in *figure 5.13*.

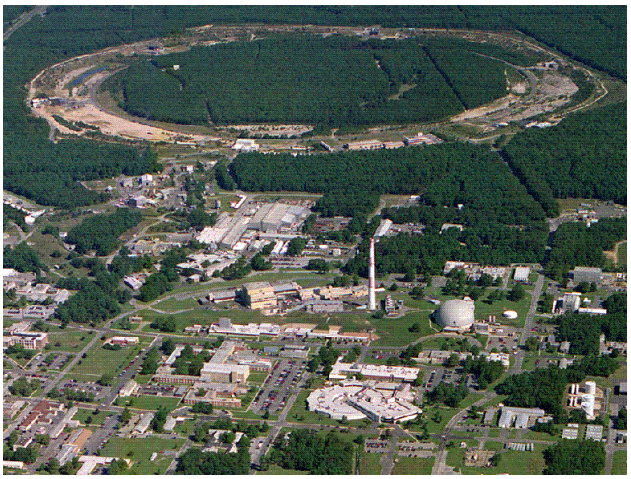

Figure 5.13: The big circle here is RHIC.

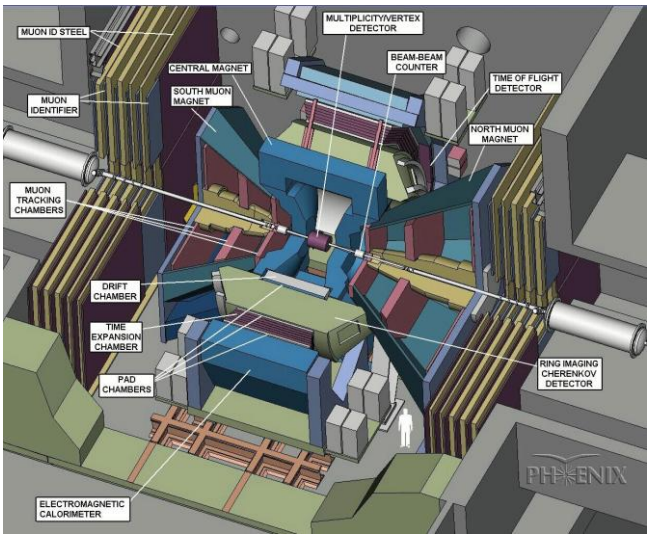

Figure 5.14: A schematic picture of the PHENIX detector.

The PHENIX detector can be divided into four smaller parts, called arms, and three kinds of detectors which surround the collision point [15], see a figure of PHENIX in *figure 5.14*. The three detectors surrounding the collision point is the Zero-Degree Calorimeters (ZDC), the Beam-Beam Counters (BB) and the Multiplicity-Vertex Detector (MVD). The ZDC detector counts the number of neutral particles (mostly neutrons from the collided nuclei) ejected from the collision. This is done by placing the detectors in the collision line (at zero degrees from the collision line) and applying a magnetic filed in front of the detector, see *figure 5.15*. Together with the BB detector, the ZDC probes how central a collision is. This is shown in *figure 5.16*, where a diagram over the energy deposit in the ZDC is plotted against the number of charge detected in the BBC. The BBC can together with the MVD also provide information about when and where the collision occurred. This is e.g. done by measuring the time-of-flight. The last detector also serves as a probe of the multiplicity.

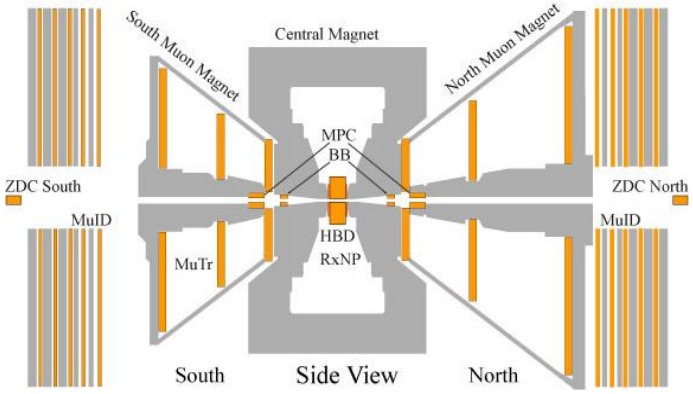

Figure 5.15: The PHENIX detector cut in the direction of the particle beam.

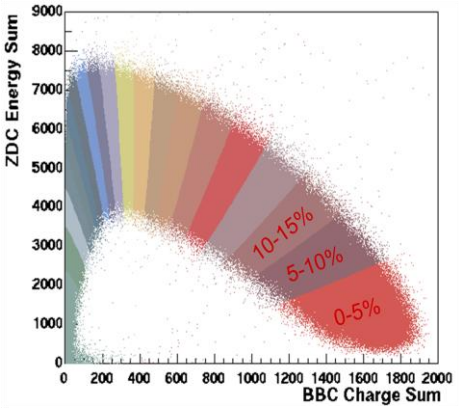

Figure 5.16: From this diagram it is possible to decide the centrality in the observed collision.

The two central arms of PHENIX consist of electromagnetic calorimeters and other detectors which detect charged particles. To get an accurate measurement of the charged particles and the photons, the calorimeters are built of lead-scintillators, while lead-glass calorimeters are used to obtain good energy resolution. To get a three dimensional track after the particles, PHENIX uses pad chambers (similar to drift chambers) rather than an ordinary TPC. The measurements here are combined with those made by a Time Expansion Chamber (special type of TPC) in the east arm. Since the detector is in a magnetic field, these tracks can be used to measure momentum. An additional way, which is used, to identify electrons is to use Ring-Image Čerenkov detectors.
The two other arms of PHENIX are used to detect muons with may emerge when J/Ψ particles decay. The south arm covers rapidities from -2.25 to -1.15 and the north rapidities from 1.15 to 2.44.

The STAR detector is, as stated before, designed to measure hadrons extremely accurate rather than photons and leptons. To get as much information as possible from every collision, it is important to combine detectors in an efficient way. One of the more important detectors is the TPC [16], which is surrounding the collision point. It is 4 meters long, has the ability to measure pseudo-rapidity in the range from -1.8 to 1.8 with full azimuthally coverage. To increase the pseudo-rapidity range of the TPC, a radial-drift TPC is incorporated as well. The energy loss resolution of the detector, which can be used to identify particles, is 7%.

Combined with the *silicon vertex tracker* (a detector which detect points where a charged particle has travelled through, compare to the MWPT) it is possible to get a very good momentum resolution.
To detect the electromagnetic interacting particles after the collisions, an electromagnetic calorimeter is surrounding the collision point. It is specifically the particles leaving the collision point in transverse direction to the beam that is interesting.
This is just some of the detectors that have made STAR as important to high energy physics as it is. Some of the others can be seen in *figure 5.17*.

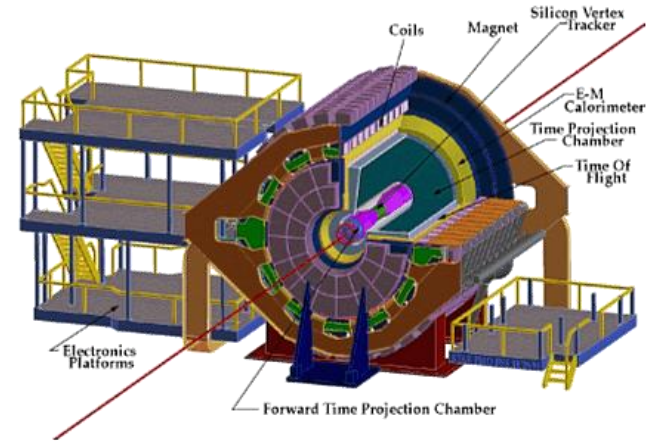

Figure 5.17: The STAR detector.

5.5 – ALICE at LHC

LHC is currently the highest energy heavy-ion collider in the world and is used to perform several different experiments. The energy ranges up to a centre-of-mass energy of 14 TeV in pp-collisions and of 5.5 TeV for Pb-Pb-collisions. One of these experiments is to investigate the QGP, which is done with the ALICE (A Large Ion Collider Experiment) experiments. Since the LHC and ALICE detectors are just a few years old, the operating energies are currently only half of the energy LHC was designed for. This is anyhow a great step in energy from the experiments that have been carried out at RHIC. The collisions are supposed to be run at maximum energy in year 2014.

The probably most important detector for ALICE is the TPC [17]. The TPC of ALICE is 5 meters long with ability to measure pseudo-rapidity between ±0.9. The energy loss resolution of the detector is said to be approximately 8-9% in a collisions with many tracks and about 5% for one single track. Together with a Transition Radiation Detector (which is an electron detector) the TPC can e.g. detect vector mesons and jets [18]. To further investigate the produced particles, other detectors are used as well. For example are velocities of the particles measured with a time-of-flight detector. To detect the muons a special muon spectrometer is used. Muons are otherwise hard to detect since they easily penetrate normal matter. Some other very important information carriers from the collisions are the photon. For the purpose of detecting these, a special detector called PHOS (PHOton Spectrometer) has been developed. This detector is very good in the range it operates, which unfortunately is limited. Outside the limits of the PHOS are, among other detectors, electromagnetic calorimeters used. These can also track jets, which of course are very important.
The detectors in ALICE can be seen in *figure 5.18*.

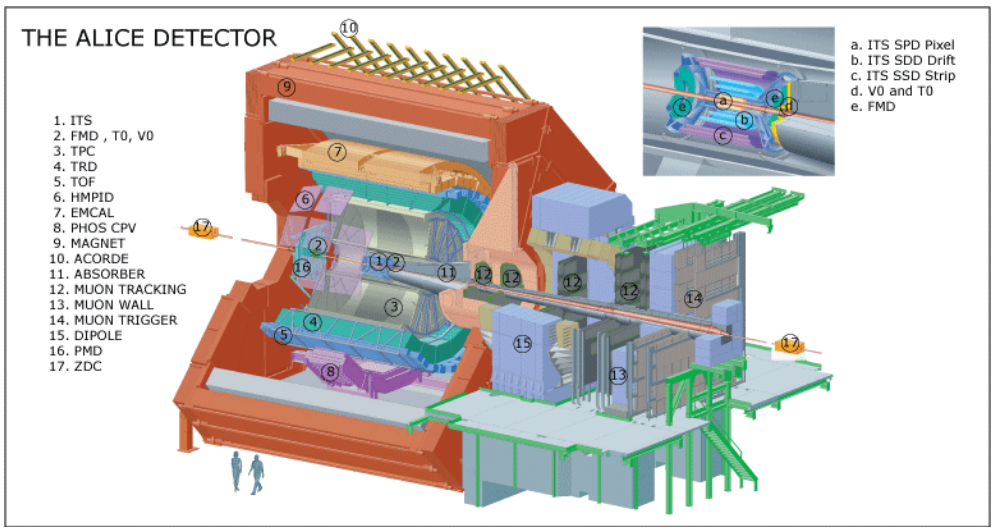

Figure 5.18: The ALICE detector at LHC.

Chapter 6.
- Results

6.1 – Introduction

At the time that this thesis is written, the energies at CERN have only reached half of the energy it is designed for. This is anyhow higher than those energies achieved at RHIC, but no new phenomena have yet been observed. The general trends from the RHIC experiments have so far been confirmed. It is possible that the situation will change as the energies at CERN increase, but as stated in the previous chapter, LHC will not operate at its maximum energy until year 2014. This chapter will thus mainly consist of observations made at BNL.
In section 4.3 we discussed some of the signals one expected to observe if an eventual QGP was present. Some of them have actually been observed, while it is debated whether others have or have not. Beside these other signals have been observed as well.

6.2- Elliptic Flow

Before the experiments at RHIC had begun, the physicists thought that the phase transition from normal nuclear matter would be to a gas of weakly coupled particles. This was however not the case. Instead the QGP produced at RHIC behaved as a *perfect liquid*, a liquid with very low viscosity. One reason for this behaviour was a phenomenon called *elliptic flow*.

To explain what elliptic flow is, let us think of a peripheral AA-collision. Let us also introduce a plane in space, called the *reaction plane*, defined as in *figure 6.1* and an angle Φ, measured in the plane orthogonal to the beam direction.

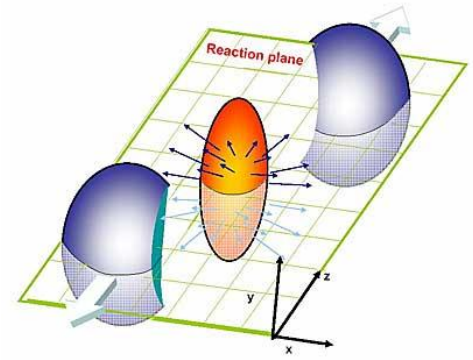

Figure 6.1: The reaction plane coincides with the x-z-plane in this figure. The angle Φ is measured in the y-x-plane.

After the collision, the dense matter in the participant region will expand in some way. Before the experiments at RHIC were started, the physicists thought that the matter would expand isotropically. This is the way a gas would behave. But what they observed was an anisotropic expansion, where more particles were ejected inside the reaction plane than perpendicular to the plane. This flow of particles would later be used to probe QGP.

The flow can be described [19] as the number of particles per transverse momentum and azimuthal angle Φ:

$$\frac{d^2N}{dP_t d\Phi}.$$

By use of the experimental data obtained from the collision it is possible to Fourier decompensate the angular part of the above expression:

$$\frac{dN}{d\Phi} = \frac{1}{2\pi}[v_0 + 2v_1\cos(\Phi - \Phi_R) + 2v_2\cos(2(\Phi - \Phi_R)) + 2v_3\cos(3(\Phi - \Phi_R)) + \cdots].$$

The angle θ_R subtracted in the argument is used to get an angle relative to the reaction plane. If all terms but the first, v_0, is 0 in the series, then no flow would be observed. The coefficient of the second term in the expansion describes an overall shift of the distribution in the momentum plane. This term is called *direct flow*. Due to symmetry, this term can be neglected at midrapidity where it according to theory should be 0 [20]. The coefficient of the second term on the other hand is very interesting. This coefficient describes the elliptic flow, or rather the eccentricity (the deviation from a circle) of an ellipse-like distribution, see *figure 6.2*. In a similar way, many of the other coefficients have a meaning. The third coefficient is e.g. a measurement of the symmetry of the collision. In a totally symmetric collision, this coefficient vanishes.

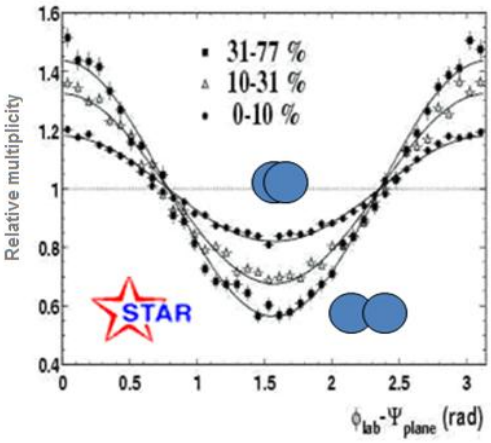

Figure 6.2: In this figure it can be seen how v_2 varies with the centrality of the collision.

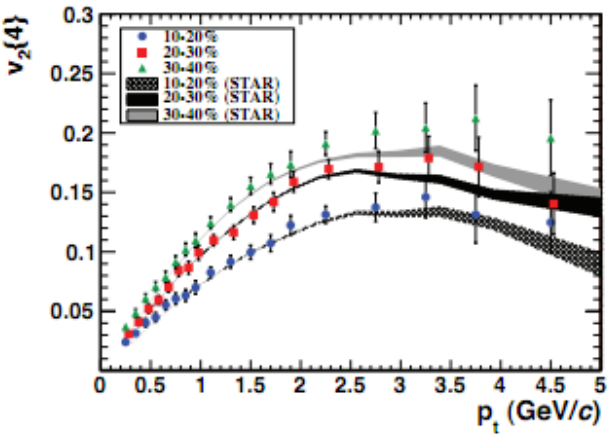

Figure 6.3: v_2 as a function of transverse momentum at different impact parameters. The figures are measurements made by ALICE, while the shaded areas are measurements made by STAR.

The reason that v_2 is an interesting observable is that it contains information about the properties of the colliding matter at very early stage. For example different values of v_2 are obtained from different values of the impact parameter. This can be seen in *figure 6.3*. What is seen there is a comparison between the graphs obtained with ALICE to those obtained with STAR. From the results obtained with the $\sqrt{s_{NN}}$ = 200 GeV Au-Au collisions at RHIC, calculations were made to predict the outcome of those that were to be made at LHC at $\sqrt{s_{NN}}$ = 2.76 Tev. These calculations were made using hydrodynamics, the dynamics treating fluids. They were consistent with the result obtained in the autumn 2010. This was a success for the interpretation of the QGP as a fluid.

The coefficient v_2 does however not only depend on the impact parameter [21]; it does also depend on the particle being observed. A very interesting observation made here is that the mesons and baryons, separately, seem to scale when the flow is studied as a function of kinetic energy. This is shown in the left part of *figure 6.4*.

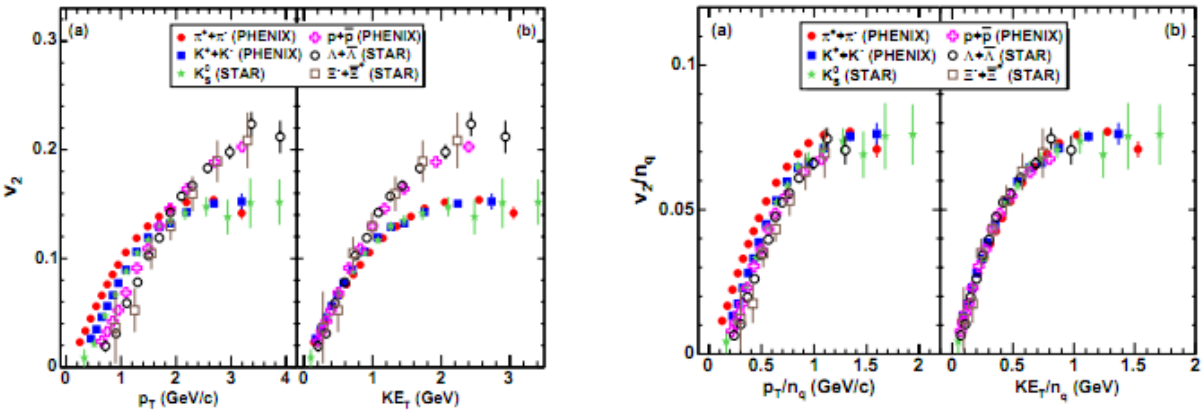

Figure 6.4: In the left figure, v_2 is plotted against the transverse momentum/kinetic energy. It is clear that the hadrons scale into baryons and mesons at higher energies. In the right figure are the parameters are divided by the relevant quark constituent. Then the hadron scaling disappears.

To the right in figure 6.3, an even more impressing scaling is observed. Here the flow parameter is divided by the number of constituent quarks and plotted versus the kinetic energy per quark. This scaling has been interpreted as a clear indication that quarks, and not the final state particles, are flowing. This supports the idea that the particles are formed by recombining quarks, rather than by fragmentation.

A characteristic property of a perfect liquid is that the ratio η/s, the viscosity divided by the entropy density, is zero. It is yet unclear if any real physical fluid actually has a ratio equal to zero or not. However, a lowest limit has, with certain assumptions, been obtained theoretically, with a result near the ratio fund at RHIC [20].

6.3 – Jet-quenching and High P_t-suppression

After the first few years at RHIC, the signals from jet-quenching and high p_t-suppression were, beside elliptic flow, two of the signals that attracted most attention [22] [23].

In *figure 6.5* the nuclear modification factor is plotted as a function of p_t. This is done for three kinds of collisions; d-Au-collisions, peripheral and central Au-Au-collisions. In the figure it is obvious that the yields in the central collisions are suppressed. The suppression is varying a bit, but R_{AuAu} appears to be approximately 0.2. For the peripheral collision it is hard to see any large suppression within the limits of the experiments accuracy. These results are more similar to those obtained from d-Au-collisions rather than those from central Au-Au-collisions.
Since the value of $R_{d\text{-}Au}$ is more or less unity, the initial effects due to shadowing or gluon saturation can be secluded as an explanation of the suppression in central Au-Au-collisions. In all of the collisions it can be seen that the graphs rises between 0 and 2 GeV. This is an effect of soft hadronic processes, which are not expected to scale in the same way. At higher

momentum, momentum between 2 and 6 GeV, the nuclear modification factor are rather enhanced than suppressed. This is due to the *Cronin effect*. This effect is also seen at lower collision energies and is believed to arise from rescattering of the produced particles.

Jet-quenching could be seen in central Au-Au-collisions at $\sqrt{s_{NN}}$ = 200 GeV, this is shown in *figure 6.6*. This data was obtained by the STAR-collaboration, where the trigger particle was set to have a transverse momentum in the range 4-6 GeV. The associated particles were searched for in range from 2 GeV and higher. ΔΦ is here the azimuthal angle relative to the trigger particle. As can be seen in the figure, most of the produced particles can be associated with either the trigger-jet or the jet going in the opposite direction. This is the case for d-Au-collisions and for peripheral Au-Au-collisions, whereas in the case of central Au-Au the away jet completely disappears. This is exactly what was expected from the discussion in section 4.3.3.

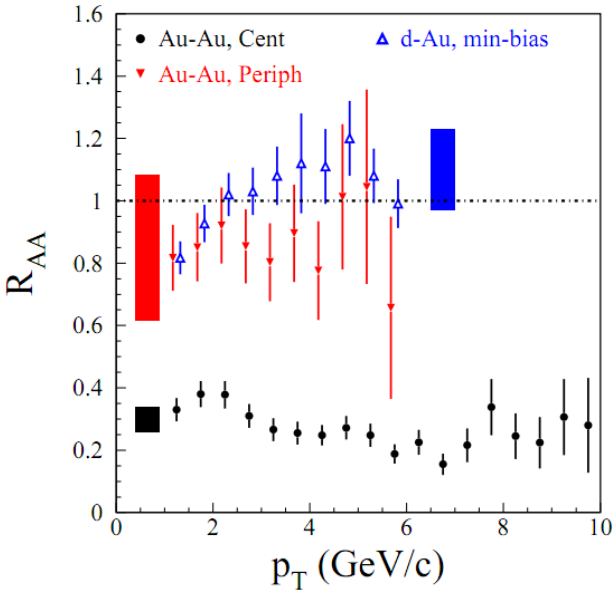

Figure 6.5: The nuclear modification factor as a function of transverse momentum.

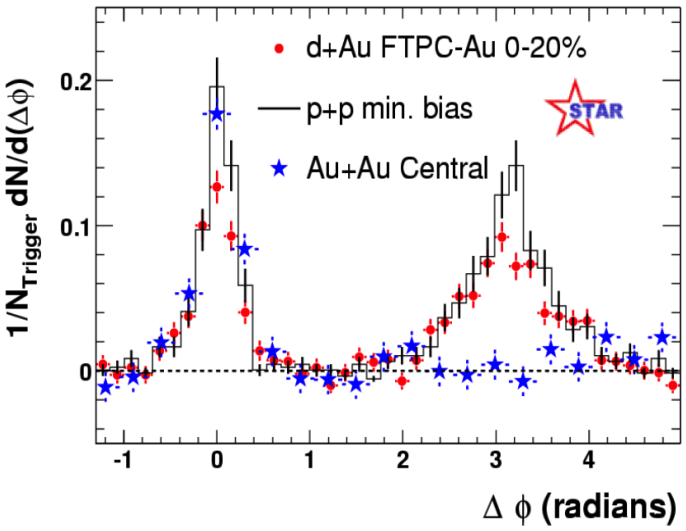

Figure 6.6: For the central Au-Au-collisions it is obvious that the away-jet has disappeared.

6.4 – J/Ψ-Suppression

Already at CERN's older facility SPS (Super Proton Synchrotron), some indication of the J/Ψ-suppression was observed [24] [25] [26]. The experiments there were made at an energy at $\sqrt{s_{NN}}$=17.3 GeV. It is debated whether the results observed here really were a first sign of the QGP. However similar experiments were later preformed at RHIC, but at higher energies, $\sqrt{s_{NN}}$=200 GeV. These results were similar to those obtained at CERN. This was quite surprising to many physicists, who thought that new information could be extracted from the higher energy densities available at RHIC. The J/Ψ-suppression has also been successfully modelled without involving any new state of matter, but extreme matter densities have to be present in such a model. Suppression of the somewhat heavier charmonium state, Ψ′, has also been studied. A similar but stronger suppression is found for the Ψ′, which is expected since the dissociation energy for the Ψ′ is lower than for the J/Ψ.

In *figure 6.7* the missing charmonium yield, relative to the expected yield, can be seen. This behaviour of the charmonia could already be seen in p-A-collisions, which in some sense questions the J/Ψ-suppression as a QGP probe. Beside, results from experiments show that the suppression of charmonia is affected by other effects apart from those due to a QGP. For example it is found that the suppression has a complicated behaviour, which among other parameters depends on the transverse momentum and centrality of the collision. New theories which try to incorporate these observations are currently being developed. Even though the mechanisms behind the suppression are not yet fully understood, it is thought that the suppression at least partly is due to a compressed form of nuclear matter formed in the collisions. Hopefully the higher energies available at LHC can give new information of how the suppression mechanism works, information which can give a hint in which direction the theorists should develop the theories.

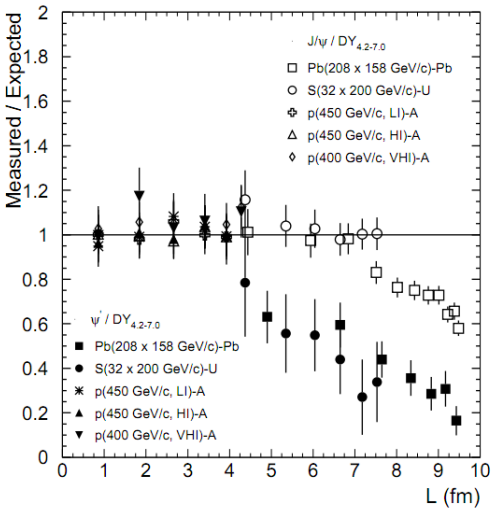

Figure 6.7: Here the ratio between the measured and expected value of the J/Ψ yield is plotted. The variable L on the horizontal axis is the average path crossed by the $c\bar{c}$ pair inside the nucleus. The energies are in fixed target mode.

6.5 – Strangeness and Charm Enhancement

After the experiments preformed at RHIC, results was obtained which could be interpreted as strangeness enhancement [27]. The observation here was, like in the other cases, seen when comparing AA-collisions scaled to pp-collisions. A large enhancement was observed at RHIC, in both gold and copper collisions. This effect was even seen in peripheral collisions. The enhancement can be seen in *figure 6.8*, where protons (uud), lambda hyperon (uds), xi hyperon (uss or dss) and omega hyperon (sss) are shown. It is easy to see that the enhancement seems to increase with the number of s-quarks the particles consists of.

It was also observed that the system size had a large impact on the enhancement, something which previous models had problems to handle. These previous models, which were based on Grand-Canonical ensemble, expected the enhancement to saturate, but this was not observed. Another surprise was that the enhancement was higher in central Cu-Cu-collisions than in peripheral Au-Au-collisions where number of participants was equal. This lead to the conclusion, that the enhancement does not scale with the geometrical parameterization of the system size. In order to take this into account newer models have been developed. Some of

these do e.g. divide the centrality dependence into a sum, where one term is proportional to the number of participants and the other to the number of binary collisions.

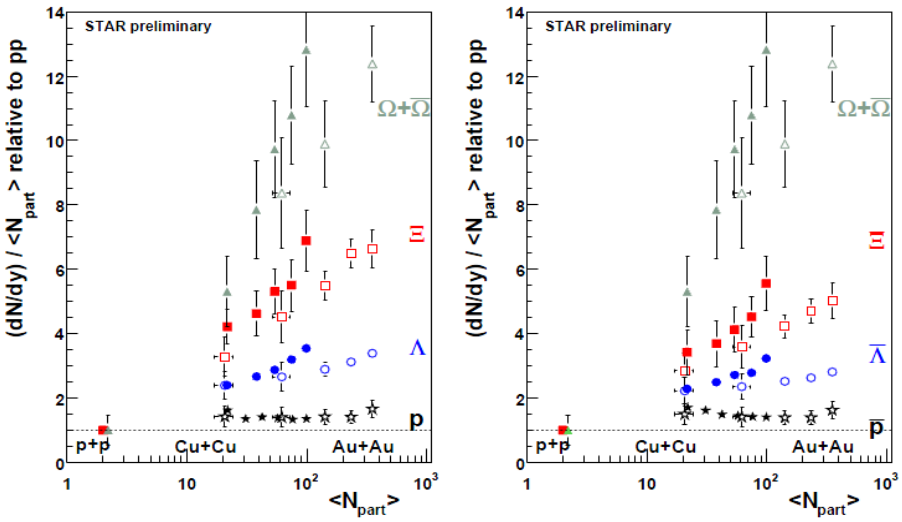

Figure 6.8: The enhancement of strange (anti-)particles.

6.6 – Summary

Many of the effects we thought we could see if a QGP was created have been seen in various experiments. It might in fact be so that the QGP was created already at SPS, where some of the signals were seen. The results seen there were later more or less confirmed by the results from RHIC. The higher energy here also allowed other phenomenon to occur. For example could the QGP be said to behave like a fluid after the experiments at RHIC. This was maybe the most unexpected result of them all. Before these results, it was thought that the QGP would be a gas rather than a fluid. If a phase transition from fluid into gas exists for the QGP is yet to be investigated. As said so many times before, let us hope that LHC can find the answers to our remaining questions.

Bibliography

1. **Nakamura, K. et al.** *Particle Data Group.* [Online] 15. January 2010. [Citeret: 31. Mars 2011.] http://pdg.lbl.gov/2010/listings/contents_listings.html.

2. **Martin, B.R. and Shaw, G.** *Particle Physics.* Chichester, West Sussex, United Kingdom : John Wiley & Sons Ltd, 2009. 978-0-470-03294-7.

3. **Jönsson, Leif.** *Particle Physics.* Lund, Sweden : n.n., 2010.

4. **Wong, Cheuk-Yin.** *Introduction to high-energy heavy-ion collisions.* Singapore : World Scientific Publishing Co. Pte. Ltd., 1994. 9810202636.

5. **Florkowski, Wojciech.** *Phenomenology of Ultra-Relativistic Heavy-Ion Collisions.* Singapore : World Scientific Publishing Co. Pte. Ltd., 2010. 978-981-4280-66-2.

6. **Smith, Roger.** *Atomic and ion collisions in solids and at surfaces.* University Press, Cambridge, UK : University of Cambridge, 1997. 0 521 44022.

7. **Kim, Eun-Joo og Yang, Hongya.** *Nuclear Modifcation Factors in d+Au and Au+Au collisions at sqrt(s)=200 Gev.* Jeonju, Republic of Korea : Chonbuk National University, 2007.

8. **Emel'yano, V., et al.** *Shadowing Effects on Particle and Transverse Energy Production.* Moscow : Moscow State Engineering Physics Institute, 1999. arXiv:hep-ph/9907367v1.

9. **Rajagopal, Krishna.** *Quark-Gluon Plasma in QCD, at RHIC and LHC, and in String Theory - Lecture 1.* Colorado : Colorado Univeristy, 2010. Video available at: http://physicslearning2.colorado.edu/tasi/tasi_2010/Videos/Rajagopal/Lecture1/Lecture1.html.

10. **Jarosik, N. et al.** Seven-Year Wilkinson Microwave Anisotropy Probe (WMAP) Observations. *NASA's data center for Cosmic Microwave Background research.* [Online] 2011. [Citeret: 8. April 2011.] http://lambda.gsfc.nasa.gov/product/map/dr4/pub_papers/sevenyear/basic_results/wmap_7yr_basic_results.pdf.

11. **Karttunen, Hannu, et al.** *Fundamental Astronomy.* New York : Springer Berlin Heidelberg, 2007. 978-3-540-34143-7.

12. **Brown, Ian G.** *The physics and technology of ion sources.* Weinheim, Germany : WILEY-VCH Verlag GmbH & Co. KgaA, 2004. 3-527-40410-4.

13. **Krane, Kenneth S.** *Introductory Nuclear Physics.* USA : John Wiley & Sons, 1988. 978-0-471-80553-3.

14. **Mitchell, Jeffery T.** An Intoduction to PHENIX. [Online] 5. 12 2008. [Citeret: 7. 5 2011.] http://www.phenix.bnl.gov/phenix/WWW/intro/.

15. **Adcox, K. , et al.** *PHENIX Detector Overview.* s.l. : Brookhaven National Laboratory, 2003. 499 469-479.

16. **Friman, Bengt, et al.** *The CBM Physics Book: Compressed Baryonic Matter in Laboratory Experiments.* Berlin : Springer, 2011. 3642132928.

17. **Barone, Maura.** *Advanced Technology & Particle Physics.* Singapore : World Scientific Pub Co Inc, 2002. 9812381805.

18. A Large Ion Collider Experiment. [Online] ALICE Collaboration, 2008. [Citeret: 9. 5 2011.] http://aliceinfo.cern.ch/Public/en/Chapter2/Page3-subdetectors-en.html.

19. **Voloshin, S. og Zhan, Y.** *Flow Study in Relativistic Nuclear Collisions by Fourier.* Pittsburg : University of Pittsburg, 1994.

20. **Aamodt, K., et al.** *Elliptic flow of charged particles in Pb-Pb collisions at 2.76 Tev.* Geneva : The ALICE Collaboration, 2010. 1011.3914v1.

21. **Adare, A., et al.** *Scaling properties of azimuthal anisotropy in Au+Au and Cu+Cu collisions at sqrt(s_NN) = 200 GeV.* Brookhaven : PHENIX Collaboration, 2007. 10.1103/PhysRevLett.98.162301.

22. **Abelev, B. I., et al.** *Identified high-pT spectra in Cu+Cu collisions at sqrt sNN=200 GeV.* Brookhaven : STAR Collaboration, 2009. arXiv:0911.3130v1.

23. **Adcox, K., et al.** *Formation of dense partonic matter in relativistic nucleus-nucleus collisions at RHIC: Experimental evaluation by the PHENIX collaboration.* Brookhaven : PHENIX Collaboration, 2005. arXiv:nucl-ex/0410003v3.

24. **Abele, B. I., et al.** *J/ψ production at high transverse momenta in p+p and Cu+Cu collisions at sqrt(s)=200 GeV.* Brookhaven : STAR Collaboration, 2009. Phys.Rev.C80:041902.

25. **Adcox, K., et al.** *Formation of dense partonic matter in relativistic nucleus-nucleus collisions at RHIC.* Brookhaven : PHENIX Collaboration, 2006. Nucl.Phys.A757:184-283.

26. **Alessandro, B., et al.** *ψ' production in Pb-Pb collisions.* Geneva : NA50 Collaboration, 2006. Eur.Phys.J.C49:559-567.

27. **Takahashi, J. og Derradi de Souza, R.** *Strangeness production in STAR.* Brazil : Instituto de Fisica Gleb Wataghin, 2008. arXiv:0809.0823v1.

References of Figures

Some of the pictures used in this thesis are constructed in a very simple way, and some of them have I made myself. Thus, these figures will not be given any references. Instead only the more advanced figures will be given references.

Figure 1.1: http://www.thefullwiki.org/Neutrino_oscillation, 2/3-2011

Figure 1.7: http://www.sciencephoto.com/images/download_lo_res.html/A142438-Two-jet_event_in_ALEPH_detector,_CERN-SPL.jpg?id=651420438, 24/2-2011

Figure 1.8: http://www.sciencephoto.com/images/download_lo_res.html?id=651420435, 24/2-2011

Figure 2.2: http://pdg.lbl.gov/2010/reviews/rpp2010-rev-structure-functions.pdf, 10/4-2011

Figure 2.5: [4]

Figure 4.4: http://francisthemulenews.wordpress.com/2010/11/26/el-jet-quenching-se-observa-por-primera-vez-en-las-colisiones-pb-pb-en-el-lhc-del-cern/, 7/4-2011

Figure 5.3: http://en.wikipedia.org/wiki/File:Geiger_Mueller_Counter_with_Circuit-en.svg, 30/4-2011

Figure 5.5: http://www.gsi.de/forschung/kp/kp1/experimente/alice/tpc/TPC_overview_e.html, 1/5-2011

Figure 5.6: http://g4education.kek.jp/pages/viewpage.action?pageId=1605905, 27/5-2011

Figure 5.8: http://nsspi-apps.ne.tamu.edu/NSEP/basic_rad_detection/index.php?course=0600, 2/5-2011

Figure 5.9: http://www.stanford.edu/group/ceramics/scintillators.html, 2/5-2011

Figure 5.10: http://rd11.web.cern.ch/RD11/rkb/PH14pp/node162.html, 4/5-2011

Figure 5.11: http://hepoutreach.syr.edu/Index/accelerator_science/accel_overview.html, 27/5-2011

Figure 5.13: http://faculty.washington.edu/trainor/gallery.html, 2011-9/5

Figure 5.14: http://www.phenix.bnl.gov/WWW/html/phenix_main.html, 2011-8/5

Figure 5.15: http://www.phenix.bnl.gov/WWW/INTEGRATION/ME&Integration/mechanical_specifications.htm, 10/5-2011

Figure 5.17: http://www.star.bnl.gov/central/experiment/, 2011-8/5

Figure 5.18: http://aliceinfo.cern.ch/Public/en/Chapter2/Chap2Experiment-en.html, 2011-8/5

Figure 6.3: [20]

Figure 6.4: [21]

Figure 6.5: [23]

Figure 6.6: Phys. Rev. Lett. 91 (2003) 072304

Figure 6.7: [26]

Figure 6.8: [27]